The Journal of Chemical Physics

RESEARCH ARTICLE | MAY 09 2024

From Liouville to Landauer: Electron transport and the bath assumptions made along the way \odot



J. Chem. Phys. 160, 184109 (2024) https://doi.org/10.1063/5.0201430









The Journal of Chemical Physics
2024 Emerging Investigators
Special Collection

Submit Today





From Liouville to Landauer: Electron transport and the bath assumptions made along the way

Cite as: J. Chem. Phys. 160, 184109 (2024); doi: 10.1063/5.0201430 Submitted: 30 January 2024 • Accepted: 18 April 2024 • Published Online: 9 May 2024









David Bialas¹ David Rvan Jorn^{2,a)}



AFFILIATIONS

- Department of Chemistry, Penn State Behrend, Erie, Pennsylvania 16563, USA
- ²Department of Chemistry, Villanova University, Villanova, Pennsylvania 19085, USA

ABSTRACT

A generalized quantum master equation approach is introduced to describe electron transfer in molecular junctions that spans both the off-resonant (tunneling) and resonant (hopping) transport regimes. The model builds on prior insights from scattering theory but is not limited to a certain parameter range with regard to the strength of the molecule-electrode coupling. The framework is used to study the simplest case of energy and charge transfer between the molecule and the electrodes for a single site noninteracting Anderson model in the limit of symmetric and asymmetric coupling between the molecule and the electrodes. In the limit of elastic transport, the Landauer result is recovered for the current by invoking a single active electron Ansatz and a binary collision approximation for the memory kernel. Inelastic transport is considered by allowing the excitation of electron-hole pairs in the electrodes in tandem with charge transport. In the case of low bias voltages where the Fermi levels of the electrodes remain below the molecular state, it is shown that the current arises from tunneling and the molecule remains neutral. However, once the threshold is reached for aligning the fermi level of one electrode with the molecular orbital, a small amount of charge transfer occurs with a negligible amount of hopping current. While inelasticity in the current has a minimal impact on the shape of the current-voltage curve in the case of symmetric electrode coupling, the results for a slight asymmetry in coupling demonstrate complete charge transfer and a significant drop in current. These results provide encouraging confirmation that the framework can describe charge transport across a wide range of electrode-molecule coupling and provide a unique perspective for developing new master equation treatments for energy and charge transport in molecular junctions. An extension of this work to account for inelastic scattering from electron-vibrational coupling at the molecule is straightforward and will be the subject of subsequent work.

Published under an exclusive license by AIP Publishing. https://doi.org/10.1063/5.0201430

I. INTRODUCTION

Understanding electron transfer processes is crucial to the continued development of several technologies ranging from energy storage^{1,2} to artificial photosynthesis^{3,4} and organic electronics.⁵ Accordingly, significant effort has been devoted to models for predicting the kinetics of electron transfer in these varied contexts. Marcus theory8 has been widely applied to describe electron transfer between an electron donor and an acceptor in a variety of systems, including light-harvesting assemblies, 9,10 photovoltaics, and other biological molecules. ^{13,14} The theory has been employed in recent years to describe currents between two electrodes bridged by single molecules and self-assembled monolayers. 15,16 Regarding electron transport in molecular junctions, Marcus theory has been invoked in the limit of high temperatures in the resonant transport

regime, where the energy level of the molecule is close to the Fermi levels of the electrodes, and hopping transport is expected. 17-20 In the off-resonant transport regime, the electron transfer is characterized by coherent tunneling described within the Landauer-Büttiker approach.^{21,22} In the Landauer model, the energy broadening of the molecular states from coupling to the electronic continua in the electrodes is taken into account through transmission functions obtained from scattering theory²³ or non-equilibrium Green's function calculations. 24 Beyond elastic scattering, transmission through a molecular junction can be accompanied by energy exchange with the vibrational degrees of freedom of the molecule, producing signatures in the current that contain information about the molecule and its orientation with respect to the electrodes.^{25–28} While inelastic electron tunneling spectroscopy²⁹⁻³² reveals additional insights into the structure of the molecular junction, more extreme cases of energy

a) Author to whom correspondence should be addressed: ryan.jorn@villanova.edu

accumulation can modify the junction itself by rupturing chemical bonds $^{33-36}$ or driving mechanical motion. 37

Inspired by both the potential applications of molecular devices³⁸ and the fundamental challenges of modeling open quantum systems, substantial attention has been given to the development of models spanning both the resonant and off-resonant transport regimes. ^{39,40} Intense focus from the chemistry and physics theory communities has led to a plethora of methods to describe energy and charge transfer in molecular devices much too diverse to adequately capture in the space allotted here. The reader is directed to several excellent reviews for further discussion;² however, some general categories of approaches will be briefly mentioned. Among these methods are those that can be considered perturbative in their handling of interactions between the electronic degrees of freedom of the molecule and the electrodes (the so-called electrode-molecule coupling) and between the scattering charges and the vibrations of the molecule (often referred to as the electron-phonon coupling; however, further distinction is required when molecular vibrations are involved that also interact with a separate phonon bath). Scattering theory approaches are conceptually simple, are computationally efficient, and have been successfully applied to describe inelastic electron transfer in molecular junctions in the off-resonant regime. 23,46-50 Other perturbative approaches, which properly account for the Fermi statistics of the electrons, include quantum master equations (QMEs)39, and nonequilibrium Green's fucntion (NEGF) calculations. 42,56-58 Generally, the former are reserved for the case of weak electron-molecule coupling and neglect level broadening, although efforts have been reported to extend these approaches to the off-resonant case by using dressed evolution operators⁵⁴ or memory functions calculated from numerically exact approaches. 59,60 With respect to the balance between molecule-electrode coupling and electron-phonon coupling, NEGF techniques have been explored to handle the strong and weak limits of both interactions.⁴² Indeed, in the absence of electron-phonon coupling, NEGF combined with density functional theory (NEGF-DFT) has become the standard for first-principles calculation of molecular conductance. 41

Naturally, concerns over the limited ranges of perturbative approaches can be alleviated by turning to numerically exact methods such as the hierarchical equations of motion (HEOM),4 multilayer multiconfiguration time-dependent Hartree (ML-MCTDH) descriptions of the system+bath, 66,67 and quantum Monte Carlo.⁶⁸⁻ These methods have been extended to consider coupling to multiple baths of Fermions and phonons exchanging charge and energy with a molecular subsystem, though often in the context of simplified model Hamiltonians.^{71,72} The cost of the numerically exact nature of these methods often comes in the form of the problems they can address, which have largely been restricted to one or two molecular states and similarly few nuclear coordinates. Advances in tensor train methods may provide a route to efficiently expand the feasibility of these methods to include additional molecular degrees of freedom. ^{73,74} It should be noted that the majority of studies discussed up to this point have focused on a small number of quantized degrees of freedom on the molecule. Within the context of electron transport, there remains a clear need for semi-classical methods that allow the inclusion of a mixture of quantized and classical nuclear degrees of freedom as might be needed to describe electrochemistry in a solvent environment.²⁰ Pioneering work along these lines includes the development of surface hopping treatments that account explicitly for the continua of electronic states^{75,76} or include the electrodes implicitly via broadened master equations.^{77,79}

Advances in theoretical methods to model molecular junctions have relied not only on pursuing approaches capable of spanning off-resonant and resonant transport, but also on exploring the connections between different techniques. These studies often begin with the Anderson–Holstein model Hamiltonian and introduce various *Ansätze* to bridge the transport regimes, i.e., weak to strong electrode coupling in the presence of a dissipative environment. ^{54,80,81} Formal connections have been made between techniques such as Green's function calculations and the driven–Liouville density matrix approach, ⁸² pseudo-particle NEGFs and surface hopping, ⁸³ and scattering techniques and NEGFs. ⁴⁸

While the development of numerically exact approaches continues and provides crucial benchmarks to new methods, there remains an opportunity for more approximate models valid across wide ranges of electrode-molecule coupling and electron-vibration coupling at the molecule. In this work, we motivate a model for electron transport through a molecular junction that builds on the connection between scattering theory and quantum master equations. Our approach is inspired by similar studies carried out in the context of gas phase molecular beam scattering84-86 and can be considered an extension of previous work by one of the authors in the off-resonant tunneling regime.⁴⁷ Our method accounts for all orders of electrode-molecule coupling and emphasizes the key assumptions made to derive Landauer's expression for current starting from the density matrix of the system and the Liouville equation. Our goal in making this connection explicit is to advance new directions for the development of quantum master equations to describe energy and charge transport valid across broad ranges of electrode and vibrational coupling strength. In this work, we shall focus on the electrode-molecule coupling and begin our discussion in Sec. II A with the general Hamiltonian for a molecule adsorbed to a metal surface. A Newns-Anderson type Hamiltonian is constructed using the familiar system-bath orbital partitioning; however, the electronic degrees of freedom are described with multi-electron configurations rather than restricting attention to a single incoming electrode orbital. We shall show that the retention of many-electron configurations leads naturally to the Pauli exclusion of scattering charges from thermally occupied electrode orbitals neglected in prior treatments. The transition from the full many electron states to the language of orbitals will be accomplished by restricting attention to single electron scattering events in what we term a single active electron Ansatz. Our present work will focus on a simple picture of a single molecular level coupled to the electrodes in the absence of vibrational coupling, although the model can be readily extended to treat the molecular nuclear degrees of freedom and will be the subject of a subsequent paper. With the system and bath degrees of freedom defined, we shall motivate a generalized quantum master equation (GQME)^{87,88} to describe the transport of electrons through the molecular bridge and derive the related current expressions in both the non-Markov and Markovian limits. Finally, we turn our attention to the connection with the Landauer expression for current and show that its derivation from our density matrix treatment requires not only the expected Markov limit but also the assumption of a binary collision approximation for the memory kernel in the GQME. This binary collision approximation was evoked previously to describe collisions between gas molecules at low densities in molecular beams^{\$4,86} and is applied in this context under the assumption of low densities of charge scatterers interacting with the molecular bridge. Having thoroughly explored the assumptions that connect the GQME to the Landauer result, this work provides the foundation for investigating how each of the assumptions can be relaxed to provide a new hierarchy of approximate equations of motion for the molecular subsystem that can be tested against exact methods in future work.

II. THEORY

A. Description of the molecular junction

The prototypical molecular junction envisioned in this work is shown in Fig. 1, where the voltage drop symmetrically displaces the left and right electrode Fermi levels. The Anderson Hamiltonian forms a logical starting point for discussing electron scattering from the molecule attached to the electrodes, and a similar Hamiltonian is developed here in the context of Hartree-Fock theory as discussed in Appendix A. Within Hartree-Fock, the notion of charge transfer between one-electron orbitals of the electrode and the adsorbate arises naturally from partitioning the system into electrode and molecular scattering regions. The single determinant description possesses the known flaws of missing electron correlation in addition to the assumption of Koopman's theorem to describe charged states of the molecule with frozen orbitals.⁸⁹ The benefit of Hartree-Fock is retention of exchange correlation, which will be vital to the subsequent discussion in Sec. II C of our modified self-energy expression. In an attempt to overcome loss of correlation, the Anderson model has been modified to include one-electron orbitals arising from Kohn-Sham density functional theory 41,61 and many-body molecular charged states. 83,90 Since the focus of this work is on the

qualitative aspects of the theory to describe energy and charge transfer in a molecular junction, the Hartree–Fock framework will be used for simplicity with extensions to more sophisticated treatments left to future studies. Combining Eqs. (A2) and (A7), the Hamiltonian describing the adsorbed molecule connected between the two electrodes is

$$\begin{split} \hat{H} &= \sum_{\gamma \in elec} \epsilon_{\gamma} (\{R_{elec}\}) \hat{c}_{\gamma}^{\dagger} \hat{c}_{\gamma} + \sum_{d \in molec} \epsilon_{d} (\{R_{molec}\}) \hat{c}_{d}^{\dagger} \hat{c}_{d} \\ &+ \sum_{\gamma,d} V_{\gamma,d} (\{R_{elec}\}, \{R_{molec}\}) \Big(\hat{c}_{\gamma}^{\dagger} \hat{c}_{d} + \hat{c}_{d}^{\dagger} \hat{c}_{\gamma} \Big) \\ &+ \sum_{I \in elec} \frac{1}{2M_{I}} \nabla_{R_{I}}^{2} + \sum_{J \in molec} \frac{1}{2M_{J}} \nabla_{R_{J}}^{2} + \sum_{I \in elec} \frac{Z_{I}Z_{J}}{|\vec{R}_{I} - \vec{R}_{J}|} \\ &+ \sum_{I,I' \in elec} \frac{Z_{I}Z_{I'}}{|\vec{R}_{I} - \vec{R}_{I'}|} + \sum_{I,I' \in molec} \frac{Z_{I}Z_{J'}}{|\vec{R}_{J} - \vec{R}_{J'}|}, \end{split}$$
(1)

where the first two terms correspond to the Fock spin orbital energies for the electrode and molecular regions, respectively, the third term represents the electronic coupling between these two subsystems, and the remaining contributions describe the nuclear degrees of freedom and their Coulomb repulsions. The dependence of the Fock spin orbital energies and the electronic coupling on nuclear coordinates is indicated explicitly by the notation in braces. However, in keeping with the Born-Oppenheimer separation, the coordinate dependence will be extracted from the orbital energies and replaced with a potential energy function in the nuclear subspace. Focusing first on the electrode nuclei, it is anticipated that for rapid relaxation of the collective electrode phonon degrees of freedom, a harmonic approximation will capture the essential physics. However, such an approximation is less justified a priori for the molecular degrees of freedom, where the nuclei can undergo largescale dynamics as a result of temporary localization of scattering charges and energy accumulation. 37,74 Accounting for the differences between these two vibrational subsystems, the Hamiltonian is

$$\begin{split} \hat{H} &= \sum_{\gamma \in elec} \epsilon_{\gamma}(\{R_{elec}^{eq}\}) \hat{c}_{\gamma}^{\dagger} \hat{c}_{\gamma} + \sum_{d \in molec} \epsilon_{d}(\{R_{molec}^{eq}\}) \hat{c}_{d}^{\dagger} \hat{c}_{d} + \sum_{\gamma,d} V_{\gamma,d}(\{R_{elec}\}, \{R_{molec}\}) \left(\hat{c}_{\gamma}^{\dagger} \hat{c}_{d} + \hat{c}_{d}^{\dagger} \hat{c}_{\gamma}\right) + \sum_{Q_{i} \in elec} \hbar \omega_{Q_{i}} \left(\hat{b}_{Q_{i}}^{\dagger} \hat{b}_{Q_{i}} + \frac{1}{2}\right) \\ &+ \sum_{J \in molec} \frac{1}{2M_{J}} \nabla_{R_{J}}^{2} + \hat{V}_{N}(\{R_{molec}\}) + \sum_{d' > \text{HOMO}} \left(\hat{V}_{N+d'}(\{R_{molec}\}) - \hat{V}_{N}(\{R_{molec}\})\right) \hat{c}_{d'}^{\dagger} \hat{c}_{d'} \\ &+ \sum_{d' \leq \text{HOMO}} \left(\hat{V}_{N-d'}(\{R_{molec}\}) - \hat{V}_{N}(\{R_{molec}\})\right) \left(1 - \hat{c}_{d'}^{\dagger} \hat{c}_{d'}\right) + \sum_{I \in elec} \frac{Z_{I}Z_{I}}{|\vec{R}_{I} - \vec{R}_{J}|}, \end{split}$$

$$(2)$$

where the states of the molecule have been partitioned into a reference neutral electronic configuration with N electrons (in the absence of an applied bias voltage), anionic states with an electron added to a spin orbital above the HOMO, i.e., (N+d'), and cationic states with an electron removed from a spin orbital equal to or lower than the HOMO in energy, i.e., (N-d'). The nuclei of the electrodes are described via phonon modes denoted by Q_i with frequencies

 ω_{Q_i} and creation/annihilation operators \hat{b}^{\dagger} and \hat{b} , respectively. In writing Eq. (2), the vibronic state space arising from the molecular region has been substantially narrowed to considering only singly ionized charged states in order to connect with previous theories focused on one electron charge transfers. The nuclear potential energy functions for the neutral state and charged states are given by $V_N(\{R_{molec}\})$, $V_{N+d'}(\{R_{molec}\})$, and $V_{N-d'}(\{R_{molec}\})$, respectively.

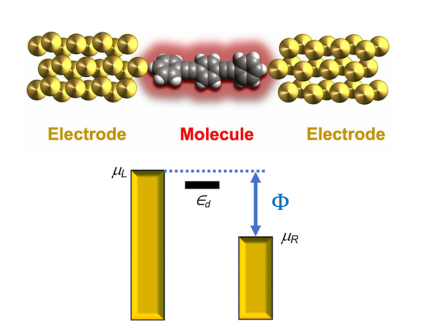


FIG. 1. A prototypical two-contact molecular junction (upper) and a simple schematic of the positions of the Fermi levels of the left and right electrodes at a positive applied bias voltage (lower). The applied voltage is indicated by Φ , and the position of the molecular state is indicated by ϵ_d .

Since it is assumed that the electrode phonon modes are not perturbed greatly by their interaction with the molecule, they can be treated as a thermal bath of a fixed temperature coupled to the molecular subsystem. This distinction invites a revision of the Hamiltonian to reflect the interaction between the vibrations of the molecule and the average behavior of the phonon bath degrees of freedom, ⁹¹

$$\hat{H} = \langle \hat{H} \rangle_{phonon} + (\hat{H} - \langle \hat{H} \rangle_{phonon}), \tag{3}$$

where $\langle \cdot \rangle_{phonon}$ denotes a thermal average across the phonon modes. The first term on the right-hand side of Eq. (3) describes the evolution of the system subject to a mean field, while the second term in parentheses captures the effect of explicit correlation between the phonon bath dynamics and the molecular system. A further simplification is made in assuming that the electronic coupling in Eq. (2) does not depend strongly on the phonon bath coordinates such that only the molecular nuclear dependence is retained. As a result of these modifications to the original Hamiltonian, a clear distinction is made between the molecular degrees of freedom and the two separate baths present in the electrodes: the bath of scattering charges and the bath of thermalized phonons,

$$\begin{split} \hat{H} &= \sum_{\gamma \in elec} \epsilon_{\gamma} \hat{c}_{\gamma}^{\dagger} \hat{c}_{\gamma} + \sum_{d \in molec} \epsilon_{d} \hat{c}_{d}^{\dagger} \hat{c}_{d} + \sum_{Q_{l} \in elec} \hbar \omega_{Q_{l}} \left(\hat{b}_{Q_{l}}^{\dagger} \hat{b}_{Q_{l}} + \frac{1}{2} \right) \\ &+ \hat{H}_{N} + \sum_{d' > \text{HOMO}} \left(\hat{H}_{N+d'} - \hat{H}_{N} \right) \hat{c}_{d'}^{\dagger} \hat{c}_{d'} \\ &+ \sum_{d' \leq \text{HOMO}} \left(\hat{H}_{N-d'} - \hat{H}_{N} \right) \left(1 - \hat{c}_{d'}^{\dagger} \hat{c}_{d'} \right) \\ &+ \sum_{\gamma, d} V_{\gamma, d} \left(\left\{ R_{molec} \right\} \right) \left(\hat{c}_{\gamma}^{\dagger} \hat{c}_{d} + \hat{c}_{d}^{\dagger} \hat{c}_{\gamma} \right) + \hat{V}_{SB}^{phonon}, \end{split} \tag{4}$$

where $\hat{V}_{SB}^{phonon} = \hat{H} - \langle \hat{H} \rangle_{phonon}$ and the molecular nuclear Hamiltonians $(\hat{H}_N, \, \hat{H}_{N+d'}, \, \text{and} \, \hat{H}_{N-d'})$ contain the mean field interaction

with the electrode nuclei. Equation (4) can be viewed from the perspective of scattering theory as the separation of the system into an asymptotic component whose free evolution is readily understood and a scattering potential,

$$\hat{H} = \hat{H}_0 + \hat{V}_{SR}^{e-mole} + \hat{V}_{SR}^{phonon}, \tag{5}$$

where \hat{H}_0 contains the first six terms of Eq. (4) and describes the uncoupled evolution of the charges and vibrations in the electrode and the molecular region. Conversely, the potentials \hat{V}_{SB}^{e-mole} and \hat{V}_{SB}^{phonon} contain the interactions between the two subsystems of the electrode and the molecule. The electronic coupling in Eq. (5) between the electrode and the molecule, \hat{V}_{SB}^{e-mole} , corresponds to the seventh term in Eq. (4).

While Eq. (4) provides the necessary ingredients to describe the electron transfer and nuclear dynamics in the molecular subspace driven by a current, we shall restrict attention in this paper to the impact of the electronic coupling term, V_{SB}^{e-mole} , and shall neglect molecular vibrations. Neglecting molecular vibrations clearly implies two assumptions: first, the potential energy surfaces present in the relevant charge states do not differ substantially from the neutral state, and, second, the electronic coupling matrix elements in Eq. (4), i.e., $V_{dy}(\{R_{molec}\})$, are independent of molecular nuclear coordinates. When one keeps in mind that highly conjugated π-cloud systems are commonly used in molecular electronics and that strong coupling between molecular orbitals and the electrode surface further delocalize charges, it is easy to envision scenarios in which these limiting cases are applicable.³⁸ Regarding the electronic coupling, intuitively, there will be a strong dependence on nuclear coordinates across the first few nanometers from the electrode surface: the farther the nuclei are from the electrode, the exponentially lower the overlap will be between the orbitals of the molecule and electrode. However, if the molecule is strongly adsorbed to the surface and does not undergo significant vibrational dynamics during current transmission, the nuclei do not explore much of the coordinate dependence of the electronic coupling. Hence, the dependence on $\{R_{molec}\}$ can be dropped from the electronic coupling. In the limit of neglecting electron-vibrational coupling, the electronic Hamiltonian reduces to the noninteracting Anderson form that will be the focus for the duration of this

$$\hat{H} = \sum_{\gamma \in elec} \epsilon_{\gamma} \hat{c}_{\gamma}^{\dagger} \hat{c}_{\gamma} + \sum_{d \in molec} \epsilon_{d} \hat{c}_{d}^{\dagger} \hat{c}_{d} + \sum_{\gamma, d} V_{\gamma, d} (\hat{c}_{\gamma}^{\dagger} \hat{c}_{d} + \hat{c}_{d}^{\dagger} \hat{c}_{\gamma}).$$
 (6)

B. Ensemble scattering theory and the equation of motion for the driven system

Having derived the Hamiltonian for the entire electrodes plus molecule system, their coupled evolution is described using the von Neumann equation, 7

$$\frac{d}{dt}|W(t)\rangle\rangle = -i\hat{\mathcal{L}}_0|W(t)\rangle\rangle - i\hat{\mathcal{V}}|W(t)\rangle\rangle,\tag{7}$$

where we assume $\hbar = 1$ throughout and $\hat{W}(t)$ is the density operator containing the complete dynamics of the electrodes plus molecule. The density operator is expressed as an extended ket $|W(t)\rangle$ in the Liouville space notation, and the reader is directed to Mukamel's classic work⁹² for further details on the connection between the Liouville space and Hilbert space representations. In Hilbert space, the evolution of the density operator results from commutation with the free Hamiltonian \hat{H}_0 as well as the scattering potential \hat{V} . However, in the Liouville notation, these operations are present in Eq. (7) via the superoperators $\hat{\mathcal{L}}_0$ and $\hat{\mathcal{V}}$, respectively. Throughout this section, tetradic operators in Liouville space will be denoted by double-hats in order to distinguish them from the Hilbert space counterparts. While Eq. (7) is entirely equivalent to the Schrödinger wave equation for the electrodes+molecule, a partitioning technique will be used to focus attention on the effect of scattering charges on the molecular degrees of freedom. Since the goal of this work is to derive effective equations of motion in which the bath degrees of freedom have been traced out, the reduced density matrix formulation provides a natural framework.

The trace over the electronic states can be readily achieved by introducing a projection operator to partition the system into a subspace of interest evolving under the influence of the electrode baths. The ubiquitous assumption of dissipative dynamics is that the equilibrium state of the bath is maintained regardless of the energy exchange with the molecular system. Such an assumption can be achieved by using the following projection defined in the basis of the eigenstates of \hat{H}_0 :

$$\hat{\hat{\mathcal{P}}} = \sum_{M,M'} |\rho_{eq}^{elec}M, M'\rangle\rangle\langle\langle M, M'|, \tag{8}$$

where the sum is over all possible electronic populations and coherences of the molecule labeled by electronic state indices, M and M', and ρ_{eq}^{selc} refers to the electrode degrees of freedom described by a thermal distribution across the electronic states. In order to account for the open system nature of the system, the electron density far from the adsorbed molecule is described by a grand canonical ensemble operator,

$$\hat{\rho}_{eq}^{elec} = \frac{\exp\left(-\beta\left[\sum_{\gamma \in R} \epsilon_{\gamma} \hat{n}_{\gamma}^{R} - \mu_{R} \sum_{\gamma \in R} \hat{n}_{\gamma}^{R}\right]\right)}{Z_{R}^{elec}} \times \frac{\exp\left(-\beta\left[\sum_{\gamma \in L} \epsilon_{\gamma} \hat{n}_{\gamma}^{L} - \mu_{L} \sum_{\gamma \in L} \hat{n}_{\gamma}^{L}\right]\right)}{Z_{c}^{elec}}, \tag{9}$$

where β is defined by the Boltzmann constant k_B and temperature T, γ is an electrode spin orbital, $\hat{n}_{\gamma}^{R(L)}$ is the number operator for the orbital, $\mu_{R(L)}$ is the fixed chemical potential for the electrode far outside of the scattering region, and the partition function is defined by

$$Z_{R(L)}^{elec} = \sum_{\{n_{\gamma}^{R(L)}\}} \left\{ \{n_{\gamma}^{R(L)}\} \middle| \exp\left(-\beta \left[\sum_{\gamma \in R(L)} \varepsilon_{\gamma} \hat{n}_{\gamma}^{R(L)} - \mu_{R(L)} \sum_{\gamma \in R(L)} \hat{n}_{\gamma}^{R(L)} \right] \right) \middle| \{n_{\gamma}^{R(L)}\} \right\}.$$
(10)

The notation $\{n_{\gamma}^{R(L)}\}$ represents a configuration of the electrode with $\sum_{\gamma \in R(L)} n_{\gamma}^{R(L)}$ electrons distributed among the electrode orbitals. Throughout this work, sums over $\{n_{\gamma}^{R(L)}\}$ imply the inclusion of all possible electrode electronic configurations with any number of total electrons.

When operating on the full density matrix, the effect of the projection operator defined in Eq. (8) is to take a trace over the electrode degrees of freedom and produce an element of the reduced density matrix pertaining to the molecular states of \hat{H}_0 ,

$$\hat{\mathcal{P}}|W(t)\rangle\rangle = \sum_{M,M'} |\rho_{eq}^{elec}M,M'\rangle\rangle\langle M| \left(\sum_{\{n_{y'}^{\prime\prime R}\}\{n_{y'}^{\prime\prime L}\}} \times \langle \{n_{y}^{\prime\prime R}\}\{n_{y'}^{\prime\prime L}\}|\hat{W}(t)|\{n_{y}^{\prime\prime R}\}\{n_{y'}^{\prime\prime L}\}\rangle\right) |M'\rangle$$

$$= \sum_{M,M'} |\rho_{eq}^{elec}M,M''\rangle\rangle\sigma^{M,M'}(t) = |\rho_{eq}^{elec}\sigma(t)\rangle\rangle, \qquad (11)$$

where the Hilbert space definition for the Liouville matrix element has been invoked and $\hat{\sigma}(t)$ is the reduced molecular density operator.

By defining a projection operator and its complement, $\hat{Q} = \hat{I} - \hat{P}$, Nakajima⁹³ and Zwanzig⁹⁴ demonstrated that an equation of motion can be written solely in terms of the \hat{P} projected subspace accounting for evolution in \hat{Q} ,

$$\frac{d}{dt}\,\hat{\mathcal{P}}|W(t)\rangle\rangle = -i\hat{\mathcal{P}}\,\hat{\mathcal{L}}_0\,\hat{\mathcal{P}}|W(t)\rangle\rangle
-\int_0^t\hat{\mathcal{P}}\,\hat{\mathcal{V}}e^{-i\,\hat{\mathcal{Q}}\,\,\hat{\mathcal{L}}\,(t-\tau)}\,\hat{\mathcal{Q}}\,\hat{\mathcal{V}}\,\hat{\mathcal{P}}|W(\tau)\rangle\rangle d\tau, \qquad (12)$$

where the projection of the system onto \hat{Q} at t = 0 is assumed to be zero and the potential, \hat{V} , does not couple the \hat{P} subspace to itself (consistent with the definitions in Sec. II A). Equation (12) is none other than the generalized non-Markovian quantum master equation for describing system-bath interactions whose solution has been reviewed in detail by Mulvihill and Geva.⁸⁷ The collection of operators in the integrand constitute the memory kernel for the system-bath interaction whose evaluation is complicated by the presence of a projection onto \hat{Q} in the time evolution operator. Various systems of equations relating the projected evolution operator to projection-free quantities in the time and frequency domains have been pursued,88 see Ref. 87 for a thorough discussion, and in what follows, we shall discuss a slightly modified approach inspired by observations from ensemble scattering theory in Liouville space. In Appendix B, we show that the memory kernel can be written using a product of the projection-free transition and Møller superoperators. To our knowledge, the connection between the memory kernel and scattering theory superoperators has not been discussed extensively in the past and represents an important formal result that may provide new opportunities for harmonizing different methods for modeling open quantum systems. The Liouville transition operator in Eq. (12) describes scattering driven by the system–bath interaction, while the Møller operators provide a type of scaling factor that accounts for the projection restriction on the evolution in Eq. (12).

Combining the results from Appendix B with Eq. (12), we obtain a non-Markovian equation of motion that remains exact as it preserves the full frequency dependence of the Fourier-transformed memory kernel,

$$\frac{d}{dt}\hat{\mathcal{P}}|W(t)\rangle\rangle = -i\hat{\mathcal{P}}\hat{\mathcal{L}}_0\hat{\mathcal{P}}|W(t)\rangle\rangle - \frac{i}{2\pi}\int_0^t d\tau \int_{-\infty}^{\infty} d\omega e^{-i\omega\tau} \times \hat{\mathcal{P}}\hat{\mathcal{T}}(\omega)\hat{\mathcal{P}}\hat{\Omega}^{-1}(\omega)\hat{\mathcal{P}}|W(t-\tau)\rangle\rangle, \tag{13}$$

where $\hat{\mathcal{T}}$ and $\hat{\Omega}$ correspond to the projection-free transition and Møller superoperators, respectively, and are defined in terms of Liouville–Green's superoperator in Appendix B. The equation of motion can be written more explicitly in terms of the reduced molecular density operator as

$$\begin{split} \frac{d}{dt}\sigma^{M,M'}(t) &= -i\omega_{M,M'}\sigma^{M,M'}(t) - \frac{i}{2\pi}\int_{0}^{t}d\tau\int_{-\infty}^{\infty}d\omega e^{-i\omega\tau} \\ &\times \langle \langle M,M'|\hat{\mathcal{T}}(\omega)\hat{\mathcal{P}}\hat{\Omega}^{-1}(\omega)|\rho_{eq}^{elec}\sigma(t-\tau)\rangle \rangle. \end{split} \tag{14}$$

For the present case, we shall follow the example of Ref. 96 and consider the Markov limit of the above expression. The elimination of the history-dependence in Eq. (14) represents an approximation based on the assumed speed of bath relaxation in comparison with the strength of the coupling to the molecular degrees of freedom.⁷ Mathematically, the Markov approximation is enforced by assuming that the Liouville matrix elements in Eq. (14) are relatively independent of frequency and selecting a representative value of ω for their evaluation, i.e., ω_0 . Extracting the transition and Møller superoperators from the frequency integral produces a delta function that collapses the history kernel. A caution should be noted that in taking the limit of $\omega \to \omega_0$, careful consideration is required when $\omega_0 = 0$. In such cases, we encountered terms for which the limit is divergent for the matrix elements themselves; however, the limit of the integral over frequency remains convergent. Such terms contribute to the memory of the system and thus were also excluded from the final matrix elements when we take the Markov limit. The subsequent Markovian master equation is given by

$$\frac{d}{dt}\,\hat{\mathcal{P}}|W(t)\rangle\rangle = -i\,\hat{\mathcal{P}}\,\hat{\mathcal{L}}_0\,\hat{\mathcal{P}}|W(t)\rangle\rangle - i\,\hat{\mathcal{P}}\,\hat{\mathcal{T}}(\omega_0)\,\hat{\mathcal{P}}\hat{\hat{\Omega}}^\dagger(\omega_0)\,\hat{\mathcal{P}}|W(t)\rangle,$$

(15)

where ω_0 will be taken as the frequency corresponding to the energy difference in the Liouville ket upon which the scattering superoperator acts, in the same manner as the parameterized transition operator in Hilbert space. Since these terms correspond to the parameterized version of the Møller operator on the frequency shell, we have replaced the inverse of the Møller operator with its

conjugate in accordance with the discussion in Appendix B. The definition of the projection operator can be used to write the Markovian equation of motion in terms of the reduced molecular density matrix.

$$\frac{d}{dt}\sigma^{M,M'}(t) = -i\omega_{M,M'}\sigma^{M,M'}(t) -i\langle\langle M,M'|\hat{T}(\omega_0)\hat{P}\hat{\Omega}^{\dagger}(\omega_0)|\rho_{aa}^{elec}\sigma(t)\rangle\rangle, \quad (16)$$

where the first term corresponds to the free coherent evolution of the molecular states and the second term contains the Liouville transition superoperator, $\hat{\mathcal{T}}(\omega_0)$, 95 describing all the scattering transitions between the eigenstates of \hat{H}_0 driven by the electrode bath degrees of freedom. Equations (14) and (15) remain exact in their treatment of the electrode–molecule coupling and provide the foundation for our approach to developing approximate equations of motion for electron transport.

Before concluding this section, we draw attention to the distinction between the projection-free transition superoperator shown in Eq. (14) and the full memory kernel shown in Eq. (12). If one were to replace the Møller operator in Eqs. (14) and (15) by unity, the first term in its perturbative expansion, the memory kernel would simply be approximated by the projection free transition superoperator. The relevance of this substitution was previously explored in the context of gas phase ensemble scattering^{85,98} and later adapted to electron transport by Sparpaglione and Mukamel. 99 As discussed by Snider,85 the use of a projection-free transition matrix corresponds to a subtle statement on how the bath interacts with the system. By keeping the projection free superoperator, scattering from bath interactions is reduced to individually coherent molecular collisions in the limit of low bath particle density. Hence, this approximation was coined a binary collision treatment in which the bath is assumed to interact with the molecular subsystem one scattering particle at a time. Indeed, this was the approach assumed by one of the authors in a previous study of electron scattering from molecular junctions in what amounts to the same binary collision approximation, 47,97 and we shall show that it is inherent in the Landauer model. While a reasonable approximation for low density gas collisions, the assumption of binary collisions is less intuitive in the case of electrode baths where one should consider not only the fully coherent collision of the molecule with individual bath particles but also the possibility of multiple bath particles scattering from the molecule during a given time interval. 96,99 Nevertheless, we shall show that this binary collision treatment is vital to deriving the Landauer expression for current from the GQME and agrees with the scattering description used to interpret the Landauer current expression.

C. Evaluation of the electronic transition matrix elements: The single active electron *Ansatz*

As outlined in Appendix B within the Markov approximation, the electronic transition matrix elements in Liouville space can be related to their Hilbert space analogs via

$$\langle \langle M, M' | \hat{T}(\omega_{0}) | \rho_{eq}^{elec} \sigma(t) \rangle \rangle = \sum_{\{n_{y}^{R}\} \{n_{y'}^{L}\}} \sum_{M''} P_{\{n_{y}^{R}\}} P_{\{n_{y'}^{L}\}} \langle M \{n_{y}^{R}\} \{n_{y'}^{L}\} | \hat{T}(E_{M''} + E_{\{n_{y}^{R}\} \{n_{y'}^{L}\}}) | M'' \{n_{y}^{R}\} \{n_{y'}^{L}\} \rangle \sigma^{M'',M'}(t)$$

$$- \sum_{\{n_{y}^{R}\} \{n_{y'}^{L}\}} \sum_{M''} P_{\{n_{y}^{R}\}} P_{\{n_{y'}^{L}\}} \langle M'' \{n_{y}^{R}\} \{n_{y'}^{L}\} | \hat{T}^{\dagger}(E_{M''} + E_{\{n_{y}^{R}\} \{n_{y'}^{L}\}}) | M' \{n_{y}^{R}\} \{n_{y'}^{L}\} \rangle \sigma^{M,M''}(t)$$

$$+ \sum_{\{n_{y}^{R}\} \{n_{y'}^{L}\}} \sum_{M'',M'''} P_{\{n_{y'}^{R}\}} P_{\{n_{y'}^{L}\}} \langle M \{n_{y}^{R}\} \{n_{y'}^{L}\} | \hat{T}(E_{M'''} + E_{\{n_{y'}^{R}\} \{n_{y'}^{L}\}}) | M'' \{n_{y}^{R}\} \{n_{y'}^{L}\} \rangle \sigma^{M'',M'''}(t)$$

$$\times \langle M''' \{n_{y}^{R}\} \{n_{y'}^{L}\} | \hat{T}^{\dagger}(E_{M'''} + E_{\{n_{y'}^{R}\} \{n_{y'}^{L}\}}) | M' \{n_{y}^{R}\} \{n_{y'}^{L}\} \rangle \sigma^{M'',M'''}(t)$$

$$\times \lim_{\eta,\eta'\to 0} \left(\frac{1}{E_{M'''} + E_{\{n_{y'}^{R}\} \{n_{y'}^{L}\}} - E_{M'} - E_{\{n_{y}^{R}\} \{n_{y'}^{L}\}} - i\eta} - \frac{1}{E_{M''} + E_{\{n_{y'}^{R}\} \{n_{y'}^{L}\}} - E_{M} - E_{\{n_{y}^{R}\} \{n_{y'}^{L}\}} + i\eta'}} \right),$$

$$(17)$$

where we have evaluated the tetradic matrix element at the frequency of the density operator upon which it acts, in accord with Eqs. (15) and (B17). The transition operators in Hilbert space, $\hat{T}(E)$, are on the energy shell and defined in terms of the electronic degrees of freedom of the electrode and molecule. $P_{\{n_p^{R(L)}\}}$ in Eq. (17) are the probabilities of finding the electrodes in a given incoming electron configuration, see Eq. (9), and $\sigma^{M'',M'''}(t)$ is an element of the reduced density matrix in the basis of molecular electronic states. The above transition matrix elements are similar to those presented in previous work; ^{46,47} however, it will be shown subsequently that recasting this problem within second quantization and accounting for the multi-electron nature of the electrodes allows us to go beyond the assumption of noninteracting electrodes often invoked in studies of the Anderson model. ¹⁰⁰

Up to this point, projection operators have been discussed within Liouville space as a means of distinguishing the electrode baths from the driven molecular subsystem. Having shifted to Hilbert space operators in Eq. (17), a new set of projections will be introduced to distinguish between different molecular states. Returning to the discussion in Sec. III A, attention will first be restricted to an incoming reference neutral state for the molecule, denoted $|N\rangle$, and charged states that are either cationic, $|N-d\rangle$, or anionic, $|N+d\rangle$, in nature. As a result, we shall define Hilbert space projections with respect to the neutral incoming state as

$$\hat{P} = \sum_{\{n_{y}^{\prime\prime R}\}, \{n_{y}^{\prime\prime L}\}} \left| N\{n_{y}^{\prime\prime R}\} \{n_{y}^{\prime\prime L}\} \right\rangle \left(N\{n_{y}^{\prime\prime R}\} \{n_{y}^{\prime\prime L}\} \right)
\hat{Q} = \sum_{\{n_{y}^{\prime\prime L}\}, \{n_{y}^{\prime\prime L}\}} \left(\sum_{d \leq \text{HOMO}} \left| N - d\{n_{y}^{\prime\prime R}\} \{n_{y}^{\prime\prime L}\} \right) \right)
\times \left(N - d\{n_{y}^{\prime\prime R}\} \{n_{y}^{\prime\prime L}\} \right| + \sum_{d > \text{HOMO}} \left| N + d\{n_{y}^{\prime\prime R}\} \{n_{y}^{\prime\prime L}\} \right)
\times \left(N + d\{n_{y}^{\prime\prime R}\} \{n_{y}^{\prime\prime L}\} \right| ,$$
(18)

where multiply charged states of the molecule have been excluded in accordance with the discussions in Sec. II A and Appendix A. Note

that in these projectors, the multi-electron nature of the electrodes is accounted for in the sense that all distributions of any number of electrons are allowed in the electrode orbitals. In our view, these projectors overcome an important limitation present in prior studies that treated the scattering electrons as a gas phase beam of electrons rather than a Fermi sea of charges in the electrodes. ⁴⁶ Given the resolution of the identity in terms of \hat{P} and \hat{Q} , the transition matrix elements in Eq. (17) require the evaluation of four types of matrix elements: $\hat{P}\hat{T}_e(E)\hat{P}, \hat{Q}\hat{T}_e(E)\hat{P}, \hat{Q}\hat{T}_e(E)\hat{Q}$, and $\hat{P}\hat{T}_e(E)\hat{Q}$. Each of these matrix elements can be written in terms of projected Green's operators, ⁹⁷

$$\hat{P}\hat{T}(E)\hat{P} = \hat{P}\hat{V}_{SB}^{e-mole}\hat{P} + \hat{P}\hat{V}_{SB}^{e-mole}\hat{Q}\hat{G}(E)\hat{Q}\hat{V}_{SB}^{e-mole}\hat{P},$$
(19)

where the scattering potential is the electronic coupling \hat{V}_{SB}^{e-mole} . The projected Green's operator contains a modified effective potential and is written as

$$\hat{Q}\hat{G}(E)\hat{Q} = \hat{Q}\left(E^{+} - \hat{H}_{0} - \hat{Q}\hat{V}_{SB}^{e-mole}\hat{P}\left(E^{+} - \hat{H}_{0}\right)^{-1} \times \hat{P}\hat{V}_{SB}^{e-mole}\hat{Q}\right)^{-1}, \tag{20}$$

where the superscript "+" implies a similar limit as that shown in Eq. (17), \hat{H}_0 is comprised of the sum over Fock orbital energies, and the remaining terms comprise the self-energy operator. The self-energy present in Eq. (20) accounts for all levels of interaction between the molecular charged states and the electrode orbitals and is clearly not diagonal in the electrode state space. As a result, the above Green's matrix remains explicitly dependent on the electrode configurations and is infinite in size. Since retaining an infinite matrix is computationally infeasible, a compromise will be struck between accounting for the multi-electron nature of the electrodes and keeping the self-energy diagonal in the electrode state space. This compromise can be shown to rely on a single active electron (SAE) Ansatz for the self-energy as discussed in Appendix C. In Appendix C, we show that the SAE treatment neglects contributions to the self-energy from the correlated transfer of multiple electrons while retaining the impact of the Pauli exclusion principle on the coupling between the continuum and the molecular orbital. As a result, the SAE *Ansatz* allows for extension of our model to account for interacting electrode electrons. Within the SAE *Ansatz*, the self-energy can be described in terms of anionic and cationic operators in the subspace of the molecule,

$$\begin{split} \hat{Q}\hat{V}_{SB}^{e-mole}\hat{P}\left(E^{+}-\hat{H}_{0}\right)^{-1}\hat{P}\hat{V}_{SB}^{e-mole}\hat{Q} \\ \xrightarrow{SAE} \sum_{\{n_{j}^{\prime\prime R}\},\{n_{j}^{\prime\prime\prime L}\}} \left|N+d',\{n_{j}^{\prime\prime R}\}\{n_{j'}^{\prime\prime L}\}\right\rangle\mathcal{E}_{d',d}^{(+)} \\ + \sum_{d,d'>\mathrm{HOMO}} \times \left(E^{+}-E_{N}-E_{\{n_{j''}^{\prime\prime R}\}\{n_{j''}^{\prime\prime L}\}}\right)\left\langle N+d,\{n_{j'}^{\prime\prime R}\}\{n_{j'}^{\prime\prime\prime L}\}\right| \\ + \sum_{\{n_{j''}^{\prime\prime R}\},\{n_{j''}^{\prime\prime\prime L}\}} \left|N-d',\{n_{j''}^{\prime\prime R}\}\{n_{j'}^{\prime\prime\prime L}\}\right\rangle\mathcal{E}_{d',d}^{(-)} \\ + d_{d'}\leq \mathrm{HOMO} \\ \times \left(E^{+}-E_{N}-E_{\{n_{j''}^{\prime\prime R}\}\{n_{j''}^{\prime\prime\prime L}\}}\right)\left\langle N-d,\{n_{j''}^{\prime\prime R}\}\{n_{j'}^{\prime\prime\prime L}\}\right|, \end{split} \tag{21}$$

where $\mathcal{E}^{(+)}$ and $\mathcal{E}^{(-)}$ are defined with respect to Eq. (C2). It should be noted that within the SAE *Ansatz*, the self-energy operator does not couple spin orbitals of different spin orientation. As a result, the projected Green's operators also do not couple different spin states of the system and the treatment of spin in our calculation leads to a trivial introduction of factors of 2 in evaluating the transition matrix elements. We shall return to this point in the discussion of the simple one-site model subsequently.

While the above self-energies look similar to the previous operators derived from standard scattering theory treatments, the inclusion of the multielectron nature of the electrodes fundamentally alters their behavior with respect to incoming electron energies. For the purpose of emphasizing this distinction, we will invoke two additional assumptions often used in the molecular conductance literature. First, we assume that the electronic coupling elements only depend on the energy of the related electrode orbital; hence, V_{id} will be replaced with $V_d^R(\epsilon_i)$. Furthermore, we shall invoke the wideband limit in which we assume that the density of electronic states in the electrodes is fairly constant across the energy range of interest. The wideband limit is used to justify dropping the energy dependence of the electronic coupling term, leaving us with constant parameters describing the coupling between each molecular spin orbital, \boldsymbol{d} , and the right/left electrode, $V_d^{R/L}$. Hence, the summations over electrode orbitals will be replaced with integrals over electronic energies, and the self-energy operators in Eq. (21) can be written as

$$\begin{split} \mathcal{E}_{d',d}^{(+)} (E^{+} - E_{N} - E_{\{\eta_{\gamma}^{\prime\prime\prime}\}\{\eta_{\gamma}^{\prime\prime\prime}\}}) \\ &\approx \left[V_{d'}^{R} V_{d}^{R} \rho_{R} \int_{E_{\min}^{R}}^{E_{\max}^{R}} \frac{1 - f_{R}(\epsilon_{j})}{E^{+} - E_{N} - E_{\{\eta_{\gamma}^{\prime\prime\prime}\}\{\eta_{\gamma}^{\prime\prime\prime}\}} - \epsilon_{j}} d\epsilon_{j} \right. \\ &+ V_{d'}^{L} V_{d}^{L} \rho_{L} \int_{E_{\min}^{L}}^{E_{\max}^{L}} \frac{1 - f_{L}(\epsilon_{l})}{E^{+} - E_{N} - E_{\{\eta_{\gamma}^{\prime\prime\prime}\}\{\eta_{\gamma}^{\prime\prime\prime}\}} - \epsilon_{l}} d\epsilon_{l} \right], \quad (22) \end{split}$$

$$\mathcal{E}_{d',d}^{(-)}(E^{+} - E_{N} - E_{\{n_{\gamma}^{\prime\prime R}\}\{n_{\gamma}^{\prime\prime L}\}})$$

$$\approx \left[V_{d'}^{R}V_{d}^{R}\rho_{R}\int_{E_{\min}^{R}}^{E_{\max}^{R}} \frac{f_{R}(\epsilon_{j})}{E^{+} - E_{N} - E_{\{n_{\gamma}^{\prime\prime R}\}\{n_{\gamma}^{\prime\prime L}\}} + \epsilon_{j}} d\epsilon_{j} + V_{d'}^{L}V_{d}^{L}\rho_{L}\int_{E_{\min}^{L}}^{E_{\max}^{L}} \frac{f_{L}(\epsilon_{l})}{E^{+} - E_{N} - E_{\{n_{\gamma}^{\prime\prime R}\}\{n_{\gamma}^{\prime\prime L}\}} + \epsilon_{l}} d\epsilon_{l}\right]. (23)$$

In our wideband limit expressions for the self-energy, the Pauli exclusion restrictions on the sums over the electrode orbitals are enforced by Fermi functions, $f(\varepsilon)$, evaluated in the limit of zero temperature. The presence of these Fermi functions is fully justified in the limit of zero temperature; however, their inclusion at finite temperature is an approximate enforcement of the Fermi statistics that agrees with our assumption of rapid thermalization in the electrodes. The density of states, ρ_{RIJ} , in the right (R) and left (L) electrodes provides a simple scaling factor within the wideband limit. The integration over energy can be split into real- and imaginary-valued contributions using a standard contour integral, 97

$$\int_{E_{\min}^{R}}^{E_{\max}^{R}} \frac{(1 - f_{R}(\epsilon_{j})) d\epsilon_{j}}{E^{+} - E_{N} - E_{\{n_{\gamma}^{\prime\prime R}\}\{n_{\gamma}^{\prime\prime L}\}} - \epsilon_{j}}$$

$$= P.V. \left\{ \int_{E_{\min}^{R}}^{E_{\max}^{R}} \frac{(1 - f_{R}(\epsilon_{j})) d\epsilon_{j}}{E - E_{N} - E_{\{n_{\gamma}^{\prime\prime R}\}\{n_{\gamma}^{\prime\prime L}\}} - \epsilon_{j}} \right\}$$

$$- i\pi (1 - f_{R}(E - E_{N} - E_{\{n_{\gamma}^{\prime\prime R}\}\{n_{\gamma}^{\prime\prime L}\}})), \tag{24}$$

where P.V. denotes the principal value for the integral in question. The first term in Eq. (24) produces a level shift, and the second term broadens the level in energy as a result of coupling between the electronic states of the molecule and the electrode. However, in contrast to previous scattering treatments, both of these quantities now depend on voltage through the presence of the Fermi functions. Justification for the incorporation of the electrode orbital occupations in the evaluation of the self-energies provides an opportunity to assess the impact of assuming noninteracting electrodes and is considered in Sec. III. Furthermore, it should be noted that the energy dependence of the self-energy accounted for in this work has an entirely different origin from the expansion beyond the wideband limit carried out by Erpenbeck et al. 101 In their work band studies, edges were introduced creating an energy dependence to the level broadening. In our case, the energy dependence arises from accounting for the multi-electron nature of the electrodes. One can envision a regime in which the voltage of the system and alignment of the molecular orbitals result in the disappearance of the lifetime all together, pushing the transition from resonance-mediated tunneling to charging of the molecule. This transition will be demonstrated in application to a simple one-site model below in Sec. III.

Although the previous discussion focused on the evaluation of $\hat{P}\hat{T}(E^+)\hat{P}$, the same approach can be used to calculate the $\hat{Q}\hat{T}(E^+)\hat{Q}$ projected operator. Previous measurements of current through molecular junctions have demonstrated the importance of accounting for charge transfer to the molecule under an applied bias voltage. ^{15,102,103} In the language of scattering theory, charge transfer is described by non-zero projections of the system onto the

Q-subspace and the introduction of charged scattering states. Hence, not only does one need to consider incoming scattering states in \hat{P} but also from \hat{Q} under finite voltage. The evaluation of the projected Green's operator for $\hat{Q}\hat{T}(E^+)\hat{Q}$ requires

$$\hat{P}\hat{G}_{e}(E)\hat{P} = \hat{P}\left(E^{+} - \hat{H}_{0} - \hat{P}\hat{V}^{e-mole}\hat{Q}(E^{+} - \hat{H}_{0})^{-1} \times \hat{Q}\hat{V}^{e-mole}\hat{P}\right)^{-1},$$
(25)

where \hat{H}_0 carries the same meaning as discussed in Eq. (20) and the self-energy contains two scattering interactions that will take the system from the P subspace and back again with respect to the incoming molecular configuration. Following the same reasoning as used in the SAE *Ansatz* for the incoming neutral state, the self-energy for the incoming charged states can be written as (see Appendix C)

$$\hat{P}\hat{V}_{SB}^{e-mole}\hat{Q}(E^{+}-\hat{H}_{0})^{-1}\hat{Q}\hat{V}_{SB}^{e-mole}\hat{P}$$

$$\stackrel{SAE}{\longrightarrow} \sum_{\{n_{\gamma''}^{\prime\prime}\},\{n_{\gamma''}^{\prime\prime}\}} |N,\{n_{\gamma''}^{\prime\prime\prime}\}\{n_{\gamma''}^{\prime\prime\prime}\}\}\Pi^{(+)}$$

$$\times (E^{+}-E_{N}-E_{\{n_{\gamma''}^{\prime\prime\prime}\},\{n_{\gamma''}^{\prime\prime\prime}\}})\langle N,\{n_{\gamma''}^{\prime\prime\prime}\}\{n_{\gamma'}^{\prime\prime\prime}\}|$$

$$+ \sum_{\{n_{\gamma''}^{\prime\prime\prime}\},\{n_{\gamma''}^{\prime\prime\prime}\}} |N,\{n_{\gamma''}^{\prime\prime\prime}\}\{n_{\gamma''}^{\prime\prime\prime}\}\rangle\Pi^{(-)}$$

$$\times (E^{+}-E_{N}-E_{\{n_{\gamma''\prime}\},\{n_{\gamma''\prime}^{\prime\prime\prime}\}})\langle N,\{n_{\gamma''}^{\prime\prime\prime}\}\{n_{\gamma'}^{\prime\prime\prime}\}|, (26)$$

where the two self-energy contributions now describe the broadening of the neutral state via scattering from the negatively (+1 electron) or positively (-1 electron) charged states, respectively. In the wideband limit.

$$\Pi^{(+)}(E^{+} - E_{N} - E_{\{\eta_{j}^{\prime\prime\prime}\}}\{\eta_{j}^{\prime\prime\prime}\})$$

$$\approx \sum_{d > \text{HOMO}} \left[(V_{d}^{R})^{2} \rho_{R} \int_{E_{\min}^{R}}^{E_{\max}^{R}} \times \frac{f_{R}(\epsilon_{j})}{E^{+} - E_{N} - \epsilon_{d} - E_{\{\eta_{j}^{\prime\prime\prime}\}}\{\eta_{j}^{\prime\prime\prime}\} + \epsilon_{j}} d\epsilon_{j} + (V_{d}^{L})^{2} \rho_{L} \right]$$

$$\times \int_{E_{\min}^{L}}^{E_{\max}} \frac{f_{L}(\epsilon_{l})}{E^{+} - E_{N} - \epsilon_{d} - E_{\{\eta_{j}^{\prime\prime\prime}\}}\{\eta_{j}^{\prime\prime\prime}\} + \epsilon_{l}} d\epsilon_{l}, \quad (27)$$

$$\Pi^{(-)}(E^{+} - E_{N} - E_{\{\eta_{\gamma}^{\prime\prime\prime}\}\{\eta_{\gamma}^{\prime\prime\prime}\}})$$

$$\approx \sum_{d \leq \text{HOMO}} \left[\left(V_{d}^{R} \right)^{2} \rho_{R} \int_{E_{\min}^{R}}^{E_{\max}^{R}} \right.$$

$$\times \frac{\left(1 - f_{R}(\epsilon_{j}) \right)}{E^{+} - E_{N} + \epsilon_{d} - E_{\{\eta_{\gamma}^{\prime\prime\prime}\}\{\eta_{\gamma}^{\prime\prime\prime}\}} - \epsilon_{j}} d\epsilon_{j} + \left(V_{d}^{L} \right)^{2} \rho_{L}$$

$$\times \int_{E_{\min}^{L}}^{E_{\max}^{L}} \frac{\left(1 - f_{L}(\epsilon_{l}) \right)}{E^{+} - E_{N} + \epsilon_{d} - E_{\{\eta_{\gamma}^{\prime\prime\prime}\}\{\eta_{\gamma}^{\prime\prime\prime}\}} - \epsilon_{l}} d\epsilon_{l} \right]. \tag{28}$$

An important difference in the self-energy for incoming charged states vs neutral states comes from the change in the Pauli exclusion restriction, which flips the occupied/unoccupied orbital Fermi functions in comparison with Eqs. (22) and (23).

Having applied the SAE Ansatz to $\hat{P}\hat{T}\hat{P}$ and $\hat{Q}\hat{T}\hat{Q}$, what remains is the consideration of the cross terms describing the transitions between the subspaces as a result of the electrode–molecule coupling, i.e., $\hat{Q}\hat{T}\hat{P}$ and $\hat{P}\hat{T}\hat{Q}$. Considering the former, it can be shown that

$$\hat{Q}\hat{T}_{e}(E^{+})\hat{P} = \hat{Q}\hat{V}_{SB}^{e-mole}\hat{P} + \hat{Q}\hat{V}_{SB}^{e-mole}\hat{P}(E^{+} - \hat{H}_{0})^{-1} \\ \times \hat{P}\hat{V}_{SB}^{e-mole}\hat{Q}\hat{G}_{e}(E^{+})\hat{Q}\hat{V}_{SB}^{e-mole}\hat{P},$$
(29)

where the same SAE Ansatz will be taken for the self-energy in the projected Green's operator. The additional $\hat{V}\hat{G}_0\hat{V}$ term appearing to the right of the projected Green's operator opens the possibility for electron–hole pair generation in the electrodes in tandem with charge transfer across the junction and thus presents an even deeper foray into the impact of interacting electrodes. While allowing this scattering channel may seem a violation of the spirit of the SAE model (since we consider two electrons being swapped between the electrode and molecule), it is critical to do so in order to provide an inelastic channel for charge transfer. This point will be discussed further in Sec. III, where we show that if one were to neglect electron–hole pair generation, only the elastic channels would remain in the absence of electron–vibrational coupling and the description would be limited to the off-resonance tunneling regime.

D. Current and the single active electron Ansatz

In this final section on our theoretical framework, we turn our attention to the expression for current through a driven molecular junction. The current can be defined as the time rate of change of the number of electrons present in one electrode of the system. We shall assume that there are only two contacts forming a minimal molecular device, see Fig. 1, and the operator to count the number of electrons in the left electrode is defined by

$$\hat{N}_L = \sum_{\gamma' \in L} \hat{n}_{\gamma'},\tag{30}$$

where the sum runs over the electrode spin orbitals. The rate of change of the expectation value of \hat{N}_L is then proportional to the current,

$$\begin{split} I(t) &= -q_e * \frac{d}{dt} \langle \langle N_L | W(t) \rangle \rangle \\ &= -q_e \sum_{\{n_\gamma^R\} \in n_{\gamma'}^L\}} \sum_M \left(\sum_{\gamma' \in L} n_{\gamma'}^L \right) \\ &\times \left[\frac{d}{dt} \langle \langle M \{n_\gamma^R\} \{n_{\gamma'}^L\}, M \{n_\gamma^R\} \{n_{\gamma'}^L\} | W(t) \rangle \rangle \right], \end{split} \tag{31}$$

where q_e is the magnitude of the electron charge. The above sums over M pertain to the electronic indices for the states of the molecule. The time rate of change for the density matrix is provided by either Eq. (14) or Eq. (15) with the modification that the projection onto

populations removes the free propagation term. For example, the non-Markovian result yields

$$\begin{split} \frac{d}{dt} \langle \langle M\{n_{\gamma}^{R}\}\{n_{\gamma'}^{L}\}, M\{n_{\gamma}^{R}\}\{n_{\gamma'}^{L}\}|W(t)\rangle \rangle \\ &= \frac{-i}{2\pi} \int_{0}^{t} d\tau \int_{-\infty}^{\infty} d\omega e^{-i\omega t} \langle \langle M\{n_{\gamma}^{R}\}\{n_{\gamma'}^{L}\}, M\{n_{\gamma}^{R}\}\{n_{\gamma'}^{L}\}| \\ &\times \hat{\mathcal{T}}_{\varepsilon}(\omega) \hat{\mathcal{P}} \hat{\Omega}_{e}^{-1}(\omega) |\rho_{ea}^{elec} \sigma(t-\tau)\rangle \rangle, \end{split} \tag{32}$$

where the full transition and Møller superoperators describing interactions with both electrode baths have been replaced with their electronic equivalents. According to Eq. (B14), the transition superoperator matrix elements will require the evaluation of six integrals. However, as discussed in Appendix D, the trace over molecular states allows us to write this expression in a more intuitive form directly related to the change in occupation of the left electrode,

$$I(t) = \frac{q_{e}}{4\pi^{2}} \int_{0}^{t} d\tau \int_{-\infty}^{\infty} d\omega e^{-i\omega t} \sum_{\substack{\{n_{y}^{R}\} \{n_{y}^{L}\} \\ \{n_{y}^{R}\} \{n_{y}^{L}\} \\ \{n_{y}^{R}\} \{n_{y}^{L}\} \\ \{n_{y}^{R}\} \{n_{y}^{L}\} \}} P_{\{n_{y}^{R}\}} P_{\{n_{y}^{R}\}} P_{\{n_{y}^{L}\}} \sum_{\mathbf{y}' \in L} \left(n_{\mathbf{y}'}^{L} - n_{\mathbf{y}'}^{L} \right) \sum_{M,M',M''} \left\{ \lim_{\eta,\eta' \to 0} \int_{-\infty}^{\infty} d\varepsilon \left[\frac{1}{\varepsilon + \omega - E_{M} - E_{\{n_{y}^{R}\}} \{n_{y'}^{L}\} + i\eta} \right] \right\} P_{\{n_{y}^{R}\}} P_{\{n_{y}^{L}\}} P_{$$

where the sum over the left electrode orbitals accounts for the change in occupation from the incoming state $(\{n_{\gamma'}^{L}\})$ to the final state $(\{n_{\gamma'}^{L}\})$. The various free Green's operators from Eq. (D7) have been written explicitly by inserting resolutions of the identity between operators evaluated at ϵ and $\epsilon + \omega$. The Markovian form of Eq. (33) is found by evaluating the superoperators at the frequency $\omega_0 = \omega_{M'M''}$, as discussed in Sec. II B,

$$\begin{split} I(t) &= -iq_{e} \sum_{\{n_{\gamma}^{R}\} \{n_{\gamma'}^{L}\}} P_{\{n_{\gamma'}^{R}\}} P_{\{n_{\gamma'}^{R}\}} P_{\{n_{\gamma'}^{R}\}} \sum_{y' \in L} \left(n_{\gamma'}^{L} - n_{\gamma'}^{\prime L}\right) \sum_{M,M',M''} \\ &\times \lim_{\eta \to 0} \left[\frac{1}{E_{M'} + E_{\{n_{\gamma'}^{R}\} \{n_{\gamma'}^{L}\}} - E_{M} - E_{\{n_{\gamma}^{R}\} \{n_{\gamma'}^{L}\}} + i\eta} \right. \\ &- \frac{1}{E_{M''} + E_{\{n_{\gamma'}^{R}\} \{n_{\gamma'}^{L}\}} - E_{M} - E_{\{n_{\gamma}^{R}\} \{n_{\gamma'}^{L}\}} - i\eta} \right] \\ &\times \left\langle M \{n_{\gamma}^{R}\} \{n_{\gamma'}^{L}\} | \hat{T}(E_{M'} + E_{\{n_{\gamma'}^{R}\} \{n_{\gamma'}^{L}\}}) | M' \{n_{\gamma'}^{R}\} \{n_{\gamma'}^{\prime L}\} \right\rangle \\ &\times \left\langle M'' \{n_{\gamma'}^{R}\} \{n_{\gamma'}^{L}\} | \hat{T}^{\dagger}(E_{M''} + E_{\{n_{\gamma'}^{R}\} \{n_{\gamma'}^{L}\}}) | M\{n_{\gamma}^{R}\} \{n_{\gamma'}^{L}\} \right\rangle \\ &\times \left\langle (M', M'') | \hat{\Omega}^{\dagger}(\omega_{0}) | \rho_{ea}^{elec} \sigma(t) \right\rangle \right). \end{split} \tag{34}$$

While the above results for the time-dependent current through the junction retain any number of electron transfers during each scattering interaction, we will restrict attention to the transfer of one electron into or out of the electrode orbitals in keeping with the SAE Ansatz discussed in Sec. II C. Within our limited state space, the addition of an electron to the left electrode can only arise from the donation of an electron from the molecule in the resonant transport regime or by direct tunneling from an orbital located in the

right electrode in the off-resonant regime. Similarly, the removal of an electron from the left electrode has to be connected to electron transfer to the molecule in the resonant regime or comes from an orbital in the right electrode via tunneling off-resonant. Since both transition matrix elements in Eqs. (33) and (34) connect the same initial and final electrode configurations, it can be shown that coherence terms between different charged states, i.e., cationic, anionic, and neutral states, are prohibited. Similarly, the SAE *Ansatz* will prevent switches in spin state for the transferred electron, leading to an additional multiplication of the current through a given orbital by a factor of 2 as shown below for the one-site model.

III. APPLICATION TO A ONE-SITE MODEL: BINARY COLLISIONS AND THE LANDAUER LIMIT

A. Elastic scattering and recovery of the Landauer picture

In order to make the connection with the Landauer formalism, we shall restrict attention to scattering involving a single anionic molecular state, $|N+d\rangle$, in which the lone electron can be either spin up or spin down. As mentioned in the conclusion of Sec. II D, the coherence terms between the neutral and charged states are eliminated within the single active electron *Ansatz*. Hence, the equation of motion for the neutral state population in the Markov limit becomes

$$\frac{d}{dt}\sigma^{N,N}(t) = -i\langle\langle N, N | \hat{\hat{T}}(\omega_0) \hat{\hat{P}} \hat{\hat{\Omega}}^{\dagger}(\omega_0) | \rho_{eq}^{elec} N, N \rangle\rangle\sigma^{N,N}(t)
- i\langle\langle N, N | \hat{\hat{T}}(\omega_0) \hat{\hat{P}} \hat{\hat{\Omega}}^{\dagger}(\omega_0)
\times | \rho_{eq}^{elec} N + d, N + d \rangle\rangle\sigma^{N+d,N+d}(t),$$
(35)

where the trace over the electron spin is also implied for the charge state population. Equation (35) is a non-trivial semi-classical rate equation as it contains products of hopping and tunneling pathways that connect the molecular populations. The first term in Eq. (35) includes the product of tetradics representing Liouville space pathways coupling the charged state to the neutral state (corresponding to hopping transport), as well as the product of tetradics connecting the neutral state to itself (corresponding to tunneling when accompanied by changes in the electrode orbital occupancies). The interpretation of the two terms in the equation of motion is more straightforward in the binary collision approximation where the Møller operators are replaced by unity (as discussed in Sec. II B). Within a binary collision treatment for the memory kernel, the two terms in Eq. (35) map readily to the two different mechanisms for charge transport in a molecular junction: off-resonant tunneling in the first term and resonant charge transfer in the second

term from hopping between the charged and neutral states of the molecule. Within the Landauer picture of electron conduction, pathways that include hopping-type transport are necessarily neglected, and as a result, we shall demonstrate that the binary approximation is necessary to connect our approach to the Landauer model.

In the binary collision treatment of the bath, our equation of motion for the neutral state population becomes

$$\frac{d}{dt}\sigma^{N,N}(t) = -i\langle\langle N, N | \hat{\mathcal{T}}(\omega_0) | \rho_{eq}^{elec} N, N \rangle\rangle\sigma^{N,N}(t)
-i\langle\langle N, N | \hat{\mathcal{T}}(\omega_0) | \rho_{eq}^{elec} N + d, N + d \rangle\rangle\sigma^{N+d,N+d}(t).$$
(36)

The evaluation of the transition superoperator matrix elements requires the evaluation of their Hilbert space counterparts. For example,

$$\langle \langle N, N | \mathcal{T}(\omega_{0}) | \rho_{eq}^{elec} N, N \rangle \rangle = \sum_{\{n_{\gamma}^{R}\} \{n_{\gamma'}^{L}\}} P_{\{n_{\gamma}^{R}\}} P_{\{n_{\gamma'}^{L}\}} \langle N \{n_{\gamma}^{R}\} \{n_{\gamma'}^{L}\} | \hat{T}_{\epsilon} \left(E_{N} + E_{\{n_{\gamma}^{R}\} \{n_{\gamma'}^{L}\}} \right) | N \{n_{\gamma}^{R}\} \{n_{\gamma'}^{L}\} \rangle$$

$$- \sum_{\{n_{\gamma}^{R}\} \{n_{\gamma'}^{L}\}} P_{\{n_{\gamma'}^{L}\}} P_{\{n_{\gamma'}^{L}\}} \langle N \{n_{\gamma}^{R}\} \{n_{\gamma'}^{L}\} | \hat{T}_{\epsilon}^{\dagger} \left(E_{N} + E_{\{n_{\gamma}^{R}\} \{n_{\gamma'}^{L}\}} \right) | N \{n_{\gamma}^{R}\} \{n_{\gamma'}^{L}\} \rangle$$

$$+ 4\pi i \sum_{j,j} T_{RR}(\epsilon_{j}) f_{R}(\epsilon_{j}) (1 - f_{R}(\epsilon_{j'})) \delta(\epsilon_{j} - \epsilon_{j'}) + 4\pi i \sum_{l,l'' \in L} T_{LL}(\epsilon_{j}) f_{L}(\epsilon_{l}) (1 - f_{L}(\epsilon_{l'})) \delta(\epsilon_{l} - \epsilon_{l'})$$

$$+ 4\pi i \sum_{j,l} T_{RL}(\epsilon_{l}) f_{L}(\epsilon_{l}) (1 - f_{R}(\epsilon_{j})) \delta(\epsilon_{l} - \epsilon_{j}) + 4\pi i \sum_{j,l} T_{LR}(\epsilon_{j}) f_{R}(\epsilon_{j}) (1 - f_{L}(\epsilon_{l})) \delta(\epsilon_{j} - \epsilon_{l}), \tag{37}$$

where additional factors of 2 have been introduced to account for the two possible spin contributions from the scattering charge. The transmission functions have been introduced in the wideband limit to simplify the notation,

$$T_{RL} = \left| \frac{V_d^L V_d^R}{\epsilon_l^+ - \epsilon_d - \mathcal{E}_{d,d}(\epsilon_l)} \right|^2.$$
 (38)

The self-energy for the charge state in the wideband limit is given by

$$\mathcal{E}_{d,d}(\epsilon_l) = \rho_R (V_d^R)^2 \int \frac{(1 - f_R(\epsilon_{j''}))d\epsilon_{j''}}{\epsilon_l^+ - \epsilon_{j''}} + \rho_L (V_d^L)^2 \int \frac{(1 - f_L(\epsilon_{l'}))d\epsilon_{l''}}{\epsilon_l^+ - \epsilon_{l''}}.$$
 (39)

The above integrals in the self-energy can be solved with an appropriate contour and, in the limit of low temperature, can be approximated by simple expressions for the level width and shift. While the transmission functions in Eq. (37) look very similar to those expected for elastic tunneling, it should be noted that the retention of the Fermi functions in the self-energy provides a correction to the assumption of noninteracting electrodes. If we remove the Fermi functions from Eq. (39), we recover the exact same form for the

self-energy in the noninteracting limit employed in prior scattering treatments and NEGF calculations, 46,100

$$\mathcal{E}_{d,d} = \Delta - i\pi\rho_L (V_d^L)^2 - i\pi\rho_R (V_d^R)^2, \tag{40}$$

where Δ is the real-valued energy shift of the molecular level and the sum of the imaginary components from the left and right electrodes provides the total width of the molecular state. The level shift evaluates to zero if the energy limits on the principal value integral are assumed symmetric and is often ignored altogether in qualitative studies

In Fig. 2, we demonstrate the impact of including the voltage dependence of the self-energy, via the Fermi functions, on the transmission functions. We assume the following values for the various parameters: the initial Fermi levels of the electrodes are set to $E_F^L = E_F^R = 2.40$ eV, and the bias voltage, Φ , between the electrodes is included by symmetrically displacing the chemical potentials of the left and right electrodes, i.e., $\mu_L = E_F^L + \frac{\Phi}{2}$ and $\mu_R = E_F^R - \frac{\Phi}{2}$. The location of the LUMO orbital, ϵ_d , is set to 2.90 eV, and the temperature is taken to be 25 K. For integrals across electron energies in the electrodes, cutoffs of 10 eV are used to represent the band limits located far from ϵ_d ; see Fig. 1. The strength of the coupling to the left electrode is accounted for by $\Gamma_L = \pi \rho_L (V_L^d)^2$ and ranges from 0.0023 to 0.04571 eV in accord with NEGF-DFT calculations on gold-fullerene–gold molecular junctions. ⁴⁶ For the moment, we

shall also assume that the molecule is coupled equally to the right electrode, that is, $\Gamma_R = \Gamma_L$, resulting in the total level broadening spanning $\Gamma \approx k_B T$ to $\Gamma > 10k_B T$ at the low temperatures considered. Figure 2 demonstrates the differences in the transmission function caused by evaluating the self-energy according to Eq. (39) vs the energy-independent form in Eq. (40). In particular, attention is drawn to the case of bias voltage near the threshold voltage for charge transfer to the molecular bridge, i.e., the onset of resonant transport. At voltages where the Fermi levels of both electrodes remain below the molecular bridge state, the width of the transmission peak is the same as that predicted from the constant self-energy expression. However, once the bias voltage pushes the left Fermi level above the molecular state (1.0 V and higher), the full width at half maximum of the transmission peak reduces by half and the

amplitude of the peak increases by a factor of 4, producing a larger transmission curve. The change in width results from the left electrode being blocked from contributing to the broadening of the charged state by the Pauli exclusion of the scattering charges. The impact of adding the Fermi functions in the self-energy is also to produce a bigger level shift that varies with the applied voltage through the Fermi functions. On a final note, the presence of the sharp feature in Fig. 2 in the 0.9 V transmission function is directly related to the zero temperature limit of the real part of the self-energy, which goes to infinity when the incoming electron energy aligns with the Fermi level of the left electrode; see Eq. (39).

Returning to the evaluation of Eq. (37), the first two transition matrix elements can be combined using the optical theorem and converted to rate expressions,

$$\begin{split} & \langle N\{n_{\gamma}^{R}\}\{n_{\gamma'}^{L}\}| \Big(\hat{T}_{e}\Big(E_{N} + E_{\{n_{\gamma}^{R}\}\{n_{\gamma'}^{L}\}}\Big) - \hat{T}_{e}^{\dagger}\Big(E_{N} + E_{\{n_{\gamma}^{R}\}\{n_{\gamma'}^{L}\}}\Big) \Big) |N\{n_{\gamma}^{R}\}\{n_{\gamma'}^{L}\}\Big) \\ &= -2\pi i \sum_{\{n_{\gamma}^{R}\}\{n_{\gamma'}^{L}\}} \Big[2\Big| \langle N\{n_{\gamma}^{R}\}\{n_{\gamma'}^{L}\}| \hat{T}(E_{N} + E_{\{n_{\gamma'}^{R}\}\{n_{\gamma'}^{L}\}}) |N\{n_{\gamma'}^{R}\}\{n_{\gamma'}^{L}\}\Big) \Big|^{2} \delta(E_{\{n_{\gamma}^{R}\}\{n_{\gamma'}^{L}\}} - E_{\{n_{\gamma'}^{R}\}\{n_{\gamma'}^{L}\}}) \\ &+ 2\Big| \langle N + d\{n_{\gamma}^{R}\}\{n_{\gamma'}^{L}\}| \hat{T}(E_{N} + E_{\{n_{\gamma'}^{R}\}\{n_{\gamma'}^{L}\}}) |N\{n_{\gamma'}^{R}\}\{n_{\gamma'}^{L}\}\Big) \Big|^{2} \delta(\epsilon_{d} + E_{\{n_{\gamma}^{R}\}\{n_{\gamma'}^{L}\}} - E_{\{n_{\gamma'}^{R}\}\{n_{\gamma'}^{L}\}}) \Big], \end{split} \tag{41}$$

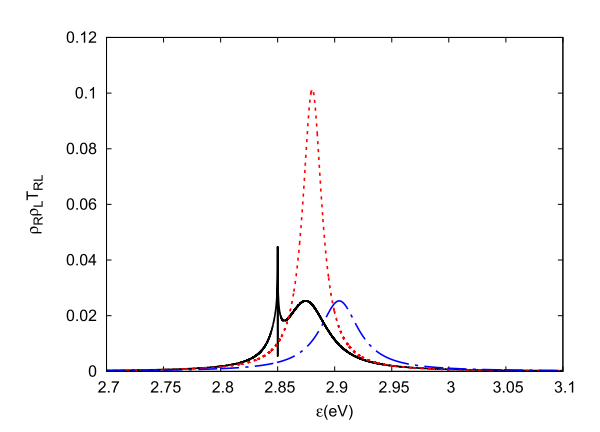


FIG. 2. Transmission function for electron transport from one side of the junction in Fig. 1 to the other with $\Gamma_L = 0.010\,35$ eV. The results are shown as a function of incoming electron energies for two different bias voltages: below resonance (0.9 V, black solid) and above resonance (1.2 V, red dotted). A comparison is also made with the transmission function using a constant self-energy that neglects bias voltage dependence (blue dotted-dashed).

where the first rate on the right-hand side of Eq. (41) corresponds to electrons tunneling from one electrode to the other and the second rate expression describes charge hopping onto the molecule. Once again factors of 2 have been added that arise from the trace over electron spin states for the scattering charge. It can be shown that the

tunneling portion in Eq. (41) cancels exactly with the contributions from the transmission functions in Eq. (37). Thus, the only contribution that produces a change in the population of the neutral state is the hopping term that transfers an electron from the electrode to the molecular bridge,

$$\begin{split} \langle \langle N, N | \mathcal{T}(\omega_0) | \rho_{eq}^{elec} N, N \rangle \rangle \\ &= -4\pi i \Big| \langle N + d \{ n_{\gamma}^R \} \{ n_{\gamma'}^L \} | \hat{T}(E_N + E_{\{n_{\gamma'}^{\ell R}\} \{ n_{\gamma'}^{\ell L} \}}) \\ &\times \left| N \{ n_{\gamma'}^{\ell R} \} \{ n_{\gamma'}^{\ell L} \} \right|^2 \delta(\epsilon_d + E_{\{n_{\gamma}^R\} \{ n_{\gamma'}^{\ell L} \}} - E_{\{n_{\gamma'}^{\ell R}\} \{ n_{\gamma'}^{\ell L} \}}). \end{split} \tag{42}$$

In the absence of additional scattering channels, such as the electron–hole pair mechanism discussed in Sec. III B, it can be shown that the above rate evaluates to zero. That these rates should be zero is confirmed by the fact that the charged state looks like a bound state of the system in the absence of any other degrees of freedom and hence should be annihilated by the application of the scattering operators. The mathematical evaluation of Eq. (42) confirms this assessment. Hence, the equation of motion for the neutral state population becomes

$$\frac{d}{dt}\sigma^{N,N}(t) = -i\langle\langle N,N|\hat{\hat{\mathcal{T}}}(\omega_0)|\rho_{eq}^{elec}N+d,N+d\rangle\rangle\sigma^{N+d,N+d}(t). \eqno(43)$$

However, the last remaining term coupling the charged state population to the neutral state can also be shown to be zero for the same reason discussed above, namely that this looks like a matrix element between bound states in the absence of additional scattering channels. As a result, for purely elastic scattering, there will be no change

in the population of the neutral or charged states of the system, and unless the molecule is initially charged, it will remain entirely neutral regardless of the applied bias voltage. This seems a curious result that independent of the voltage applied to the system, the molecule never becomes charged but is consistent with the limitation of the Landauer model to only describing electron tunneling currents in the off-resonant regime.

Given that the density matrix does not change and remains 1 in the neutral state and 0 in the charged state, the expression for current becomes

$$\begin{split} I &= -4\pi q_{e} \sum_{\{n_{\gamma}^{R}\}\{n_{\gamma}^{L}\}} P_{\{n_{\gamma}^{\prime R}\}} P_{\{n_{\gamma}^{\prime L}\}} \sum_{\gamma' \in L} \left(n_{\gamma'}^{L} - n_{\gamma'}^{\prime L} \right) \\ &+ \left[n_{\gamma}^{R} + n_{\gamma'}^{L} \right] \\ &\times \left| \left\langle N\{n_{\gamma}^{R}\}\{n_{\gamma'}^{L}\} \middle| \hat{T}(E_{N} + E_{\{n_{\gamma}^{\prime R}\}\{n_{\gamma'}^{L}\}}) \middle| N\{n_{\gamma}^{\prime R}\}\{n_{\gamma'}^{\prime L}\} \right) \right|^{2} \\ &\times \delta(E_{\{n_{\gamma}^{R}\}\{n_{L'}^{L}\}} - E_{\{n_{\gamma}^{\prime R}\}\{n_{\gamma'}^{\prime L}\}}), \end{split} \tag{44} \end{split}$$

where an additional factor of 2 has been included to account for the two different electron spins that can be transferred through the molecule. Having expressed the current in terms of the differences in occupation of the left electrode before and after the charge scattering, we can limit attention to the two transmission functions that describe electron transfer from right to left (+1 electron to the left) and from left to right (-1 electron to the left). The summation in Eq. (44) reduces to similar expressions as those found in the final two terms of Eq. (37), weighted by ± 1 for the T_{RL} and T_{LR} terms, respectively. Converting the summation over electrode orbitals to integrals over energy, we regain the familiar Landauer form,

$$I = 4\pi q_e \int d\epsilon_l \rho_R \rho_L \mathsf{T}_{RL}(\epsilon_l) (f_L(\epsilon_l) - f_R(\epsilon_l)). \tag{45}$$

However, as pointed out for the transmission function in Fig. 2, the retention of the voltage dependence of the self-energy provides a

quantitative modification from the purely noninteracting electrode model. As shown in Fig. 3, the expected current is now approximately twice that given by the noninteracting self-energy of Eq. (40). The increase in current is directly related to the observed growth of the transmission peak when the left broadening is removed from the self-energy above 1.0 V, increasing the area under the curve by an overall factor of 2.

In summary, we have demonstrated the connection between our framework and the Landauer approach to current transmission in molecular devices. In so doing, we have emphasized how our work connects with previous discussions and improves upon them. Namely, we have explored the impact of accounting for Pauli exclusion of electrons in the electrodes and the simplest extension beyond a fully noninteracting electrode model. In addition, we have emphasized that the reduction to the Landauer picture not only requires the assumption of elastic scattering through the junction but also carries an inherent assumption about the system-bath interaction, which may not be valid across a wide range of parameter space. Hence, while efforts to extend the Landauer picture to inelastic scattering are important, they likely miss additional impacts of the strong system-bath interaction arising from the treatment of the full memory kernel in a many-electron picture. The impact of the inelasticity will be explored subsequently in the Markov limit.

B. Beyond Landauer: Binary collisions with inelastic scattering

Here, we explore the impact of including an inelastic channel for charge transport: electron-hole pair excitations in the electrodes coupled to charge transfer. For positive applied bias voltages, there are two scenarios considered in Fig. 4. In the case of transitioning from the neutral state of the molecule to the charged state, an electron-hole pair is generated in the left electrode by virtue of two charge transfers between the electrode and molecule. In the second

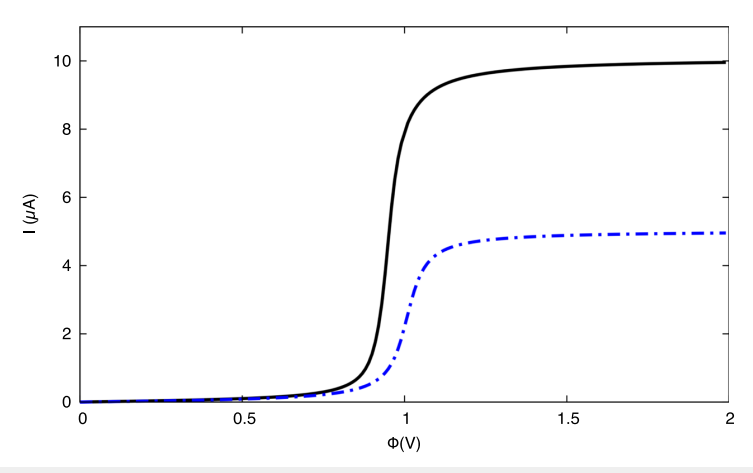


FIG. 3. Current–voltage characteristics calculated with the Landauer formula, Eq. (45), using the self-energy expression with the Fermi functions (black solid) and without consideration of the Fermi functions in the self-energy (blue dotted-dashed).

case, a transition from the charged state back to the neutral state is allowed by creating an electron-hole pair in the right electrode that absorbs some of the energy from the scattered electron. It is important to note that this mechanism of electron-hole pair generation is distinct from nonadiabatic excitation of electron-hole pairs from the nuclear motion of the molecule⁷⁶ and is unlikely to effectively compete with nonadiabatic effects in the presence of strong vibrational coupling. Nevertheless, in the absence of electron-vibrational

coupling, the inclusion of this inelastic channel warrants consideration as it changes the evolution of the molecular subsystem and points to the general impact of inelasticity in our framework. In order to accommodate electron–hole pair excitation, we shall retain our use of the SAE *Ansatz* for the projected Green's operators in the relevant transition matrix elements but shall extend the description by allowing a second electron to be exchanged in the final electrode configurations,

$$\hat{Q}\hat{T}_{e}(E^{+})|N,\{n_{\gamma}^{\prime R}\}\{n_{\gamma^{\prime}}^{\prime L}\}\rangle = \sum_{j \in R} \langle N + d\{n_{\gamma}^{\prime R} - j\}\{n_{\gamma^{\prime}}^{\prime L}\}|\hat{T}_{e}(E_{N} + E_{\{n_{\gamma}^{\prime R}\}\{n_{\gamma^{\prime}}^{\prime L}\}})|N,\{n_{\gamma}^{\prime R}\}\{n_{\gamma^{\prime}}^{\prime L}\}\rangle
+ \sum_{l \in L} \langle N + d\{n_{\gamma}^{\prime R}\}\{n_{\gamma^{\prime}}^{\prime L} - l\}|\hat{T}_{e}(E_{N} + E_{\{n_{\gamma}^{\prime R}\}\{n_{\gamma^{\prime}}^{\prime L}\}})|N,\{n_{\gamma}^{\prime R}\}\{n_{\gamma^{\prime}}^{\prime L}\}\rangle
+ \sum_{j,j',j'' \in R} \langle N + d\{n_{\gamma}^{\prime R} - j + j' - j''\}\{n_{\gamma^{\prime}}^{\prime L}\}|\hat{T}_{e}(E_{N} + E_{\{n_{\gamma}^{\prime R}\}\{n_{\gamma^{\prime}}^{\prime L}\}})|N,\{n_{\gamma}^{\prime R}\}\{n_{\gamma^{\prime}}^{\prime L}\}\rangle
+ \sum_{l,l',l'' \in L} \langle N + d\{n_{\gamma}^{\prime R}\}\{n_{\gamma^{\prime}}^{\prime L} - l + l' - l''\}|\hat{T}_{e}(E_{N} + E_{\{n_{\gamma}^{\prime R}\}\{n_{\gamma^{\prime}}^{\prime L}\}})|N,\{n_{\gamma}^{\prime R}\}\{n_{\gamma^{\prime}}^{\prime L}\}\rangle,$$
(46)

where the transition matrix elements now connect an incoming neutral molecular state with a charged state. The first two terms on the right-hand side of Eq. (46) vanish, as discussed in Sec. III A, but the latter two contributions persist and allow for population transfer. The electron–hole pair rates will carry a strong dependence on the bias voltage as a result of containing three Fermi functions arising from the electrode configuration probabilities, $P_{\{n_i^{p'}\}}$ and $P_{\{n_i^{p'}\}}$

and the repeated application of \hat{V}_{SB}^{e-mole} . The implied triple integrals in Eq. (46) can be simplified by invoking the low temperature limit of the Fermi functions as step functions. For example, when $\Phi > 0$, $E_F^I > \epsilon_d$, and $E_F^R < \epsilon_d$, we find

$$\begin{split} \left\langle \left\langle N+d,N+d\right| \hat{\hat{T}}_{e} | \rho_{eq}^{elec} N,N \right\rangle \right\rangle &\approx 8\pi i (\rho_{L})^{3} \left(V_{d}^{L}\right)^{2} \int d\epsilon_{l} f_{L}(\epsilon_{l}) \\ &\times \mathsf{T}_{LL}(\epsilon_{l}) \Bigg(\frac{1}{E_{F}^{L}-\epsilon_{l}} - \frac{1}{E_{F}^{L}-\epsilon_{d}} \Bigg). \end{split} \tag{4}$$

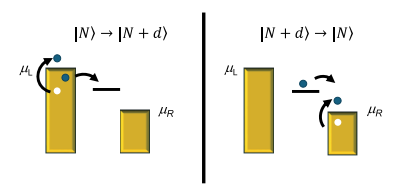


FIG. 4. Diagrams for the generation of electron–hole pairs in the electrodes concomitant with electron transfer to (left panel) or from (right panel) the molecule represented by the single site in the middle. In both cases, the left and right electrodes are filled to their respective Fermi levels as determined by their chemical potentials, μ_1 and μ_R , respectively.

A factor of 4 is introduced in the rate expression above when tracing out the various spin contributions from the two electrons involved from the left electrode. The integrals over the left electrode orbital energies preceding Eq. (47) evaluate to zero when the bias is insufficient to create the resonance condition, i.e., $E_F^L < \epsilon_d$. A similar expression to Eq. (47) can be shown for electron–hole pair generation in the right electrode when the bias voltage is reversed such that $\Phi < 0$ and the right electrode Fermi level is higher than the molecular level. Thus, between both electrodes, there are rates of charge transfer to the neutral molecular subspace that are activated by different bias voltage conditions. The rates are zero for the incoming neutral state whenever both the Fermi levels are below the charged state energy. However, once one of the Fermi levels crosses the molecular level, the channel is opened and charge exchange is allowed.

Similar results to Eq. (47) can be obtained for the charged incoming scattering state of the molecule; see the right panel of Fig. 4. In this case, the electron transferring off of the molecule loses energy to the generation of electron–hole pairs if the Fermi level resides below ϵ_d . Naturally, the ordering of the Fermi functions invoked changes in comparison with the description of the left panel in Fig. 4 and, as a result, so too does the nature of the bias voltage dependence. The rates for electron transfer from the incoming charged molecule to the electrodes will be zero if the Fermi levels are both above the bridge orbital since the inelastic channel only becomes available when excitations from below the Fermi level are allowed and there are unoccupied electrode orbitals near the bridge level. For example, when $\Phi > 0$, $E_F^R < \epsilon_d$, and $E_F^L > \epsilon_d$,

$$\begin{split} \left\langle \left\langle N,N\right| \hat{\mathcal{T}}_{e} \middle| \rho_{eq}^{elec} N + d,N + d \right\rangle \right\rangle &\approx 4\pi i (\rho_R)^3 (V_d^R)^2 \int d\epsilon_j (1 - f_R(\epsilon_j)) \\ &\times \mathsf{T}_{RR}^d(\epsilon_j) \left(\frac{1}{E_F^R - \epsilon_d} - \frac{1}{E_F^R - \epsilon_j} \right), \end{split} \tag{48}$$

where the transmission function for the charged state looks very similar to Eq. (38), albeit with the appropriately changed self-energy function.

$$\mathsf{T}_{RR}^{d} = \left| \frac{V_d^R V_d^R}{\epsilon_d - \epsilon_i^+ - \Pi(\epsilon_i)} \right|^2. \tag{49}$$

As shown in Fig. 5, the behavior of the charged state transmission functions differs from those of the neutral state with respect to changes in the applied bias voltage. In the reverse of the neutral state case, the charged state transmission depends on the self-energy of the neutral state and only allows broadening by coupling to occupied electrode orbitals. The physics is the same as the broadening of the charged state discussed in Sec. III A, namely it is the coupling of the molecular state to the continuum that gives rise to the finite level energy width. However, in this case, the broadening is caused by electron transfer to the molecule rather than from it. Hence, when the Fermi level of the electrode is above the molecular orbital, it can contribute to the broadening, but when it is below the molecular orbital, it cannot; see Eq. (27). When both the Fermi levels are below ϵ_d , the broadening vanishes entirely and the charge state represents a true bound state of the system and would produce a singularity in the transmission function. The changes in broadening with applied bias voltage are shown in Fig. 5, where at voltages above resonance, $E_F^L > \epsilon_d$, the left electrode can contribute to the broadening and produced a well-behaved peak. However, at voltages below resonance, the broadening only comes from the tail of the Fermi function that declines exponentially with bias and thus begins to approach a true singularity. In comparison with the constant self-energy result, the peak at 1.2 V differs in a manner similar to that seen in the case of the neutral transmission peak in Fig. 2, namely it is narrower and of larger amplitude than the predicted function if the Fermi statistics in the electrodes are ignored.

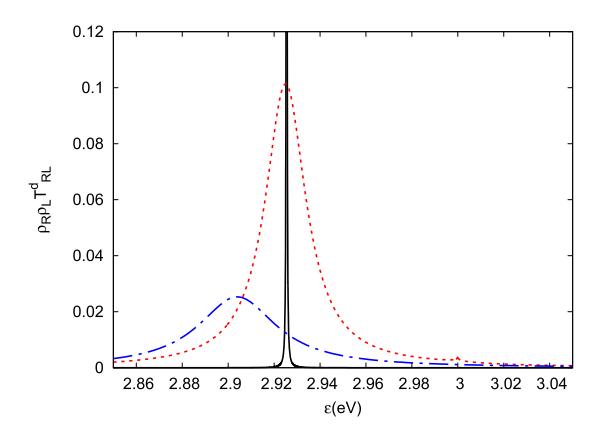


FIG. 5. Transmission function for electron transport via the charged state of the molecule with $\Gamma_R=\Gamma_L=0.010\,35$ eV. The results are shown as a function of incoming electron energies for two different bias voltages: below resonance (0.9 V, black solid) and above resonance (1.2 V, red dotted). The result for 0.9 V has been scaled by a factor of 1000 for graphing purposes. A comparison is also made with the transmission function using a constant self-energy that neglects bias voltage dependence (blue dotted-dashed).

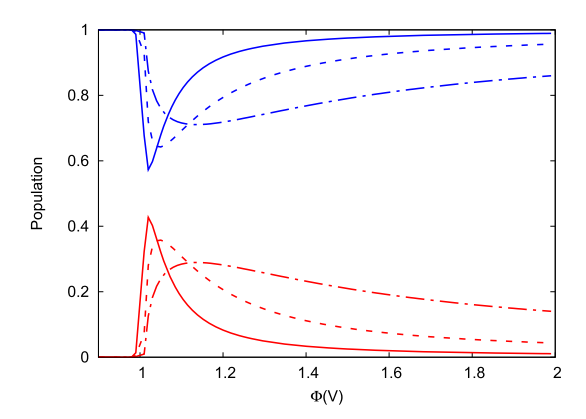


FIG. 6. Population transfer between the neutral (blue) and anionic (red) charged states of the molecule as a function of applied voltage for $\Gamma_R = \Gamma_L = 0.0023$ eV (solid), 0.010 35 eV (dashed), and 0.045 71 eV (dotted-dashed).

Having derived rate expressions for the charge transfer between the molecule and the electrodes, the evolution of the molecular density matrix simplifies to propagating two coupled differential equations for the molecular populations. While integrating the equations of motion can be carried out with standard Runge-Kutta methods, the dynamics approaching the steady state show relatively monotonic changes in state populations. As such, we restrict attention in Fig. 6 to the final steady-state populations of the neutral and charged states as a function of applied bias voltage and the electrode-molecule coupling strength. Following our observation that the inelastic channel only activates at the threshold condition $(E_F^L > \epsilon_d)$, the populations of the neutral and charged state remain unchanged up to 1.0 V. Once resonance is reached with the molecular level, the amount of charge transferred to the molecule depends on the competition between the rates discussed previously in Eqs. (47) and (48). For all three coupling strengths considered in Fig. 6, an initial transfer of charge to the molecule at threshold decays with increasing voltage. The reason for the drop off in population transfer with bias is demonstrated in comparing the different behaviors of the two processes in Fig. 4. The rate for electron transfer from the molecule results from electron-hole pairs generated in the right electrode and includes all the possible excitations that range from 0 to $\epsilon_d - E_F^R$. As the bias increases and pushes E_F^R lower, the window of available electron-hole pair excitations expands and the rate increases. In contrast, the rate for charge transfer to the molecule is supported by electrons with energy between that of the molecular level and the Fermi level of the left electrode. The energy range from ϵ_d to E_F^L will remain much smaller than that of the right electrode process. In the case of the smallest coupling, this disparity in integration ranges is offset by the sharpness of the resonance peak, which is well captured even within the smaller range selected in the left electrode and produces the largest initial transfer to the molecule. As the level broadening increases with increasing coupling strength, the transmission functions present in Eqs. (47) and (48) show a more gradual variation in the relevant integration ranges, and, hence, the changes in the amount of population transfer are more gradual as a function of bias voltage. From consideration of the behavior of the rates for charge transfer, the symmetric nature of the coupling to the right and left electrodes argues for the lack of charge buildup on the molecule. We shall show in Sec III C that breaking this symmetry gives rise to more substantial and sustained population transfer to the charged state.

Given the steady-state populations as a function of bias voltage, we now turn to the behavior of the current beyond the limit of elastic transmission. Starting from Eq. (34), the current retains the Landauer terms discussed in Sec. III A but now also accounts for charge transfer to and from the molecular subspace,

$$\begin{split} I(t) &= 4\pi q_e \int d\epsilon_l \rho_R \rho_L \mathsf{T}_{RL}(\epsilon_l) \big(f_L(\epsilon_l) - f_R(\epsilon_l) \big) \sigma_{N,N}(t) \\ &+ 4\pi q_e \int d\epsilon_l \rho_R \rho_L \mathsf{T}_{RL}^d(\epsilon_l) \big(f_L(\epsilon_l) - f_R(\epsilon_l) \big) \sigma_{N+d,N+d}(t) \\ &+ 8\pi q_e \big(\rho_L \big)^3 \big(V_d^L \big)^2 \int d\epsilon_l f_L(\epsilon_l) \mathsf{T}_{LL}(\epsilon_l) \\ &\times \left(\frac{1}{E_F^L - \epsilon_l} - \frac{1}{E_F^L - \epsilon_d} \right) \sigma_{N,N}(t) - 4\pi q_e \big(\rho_L \big)^3 \big(V_d^L \big)^2 \\ &\times \int d\epsilon_l \big(1 - f_L(\epsilon_l) \big) \mathsf{T}_{LL}^d(\epsilon_l) \bigg(\frac{1}{E_F^L - \epsilon_l} - \frac{1}{E_F^L - \epsilon_d} \bigg) \sigma_{N+d,N+d}(t), \end{split}$$

where the first two terms correspond to off-resonant scattering and the third and fourth terms correspond to redox processes. At the positive bias voltages considered, the final term in Eq. (50) does not contribute. The identification of the various terms by their scattering description provides a natural decomposition of the current into coherent tunneling and the sequential hopping mechanisms. Figure 7 shows the results for current through the symmetrically coupled molecular junction and the evolution of the contributions from the various terms in Eq. (50). Clearly, below resonance with

the molecular level, the current arises solely from coherent scattering involving the neutral state. However, once the Fermi level of the left electrode reaches the molecular orbital, population transfer occurs between the neutral and charged states and the current now arises from the sum of coherent tunneling via both routes. Since the molecule is symmetrically coupled to the two electrodes, the overall shape of the current–voltage curve does not differ substantially from that seen in Fig. 3. The contribution from the electron hopping term is shown in the inset of Fig. 7 and remains orders of magnitude smaller than the two coherent tunneling contributions. The reason for the disparate magnitudes in these contributions arises from the differing powers of electrode–molecule coupling present in the transition matrix elements for electron–hole pair creation $(V_{R/L}^3)$ vs elastic tunneling $(V_{R/L}^2)$.

In summary, we have illustrated the impact of inelastic scattering within the binary collision approximation as a first look at transport beyond the Landauer picture. By inclusion of electron-hole pair generation with the charge transmission, we have seen the onset of charge transfer to the molecule as the bias voltage pushes the left electrode's Fermi level past the molecular orbital. Hence, our framework captures both limits of charge tunneling through the molecule and charge transfer to the molecule.

C. Asymmetric coupling and molecular charge transfer

As a final test case, we also consider the impact of varying the coupling between the left and right electrodes. In this asymmetric junction, the coupling to the right electrode was reduced as compared to the left by factors of 2, 5, and 10, i.e., $V_d^L/V_d^R=2$, 5, 10. Beyond a simple numerical exercise, such a difference in coupling strengths could be reflective of molecular junctions formed in scanning tunneling microscope experiments and in self-assembled monolayers where the molecule is chemisorbed to one electrode and

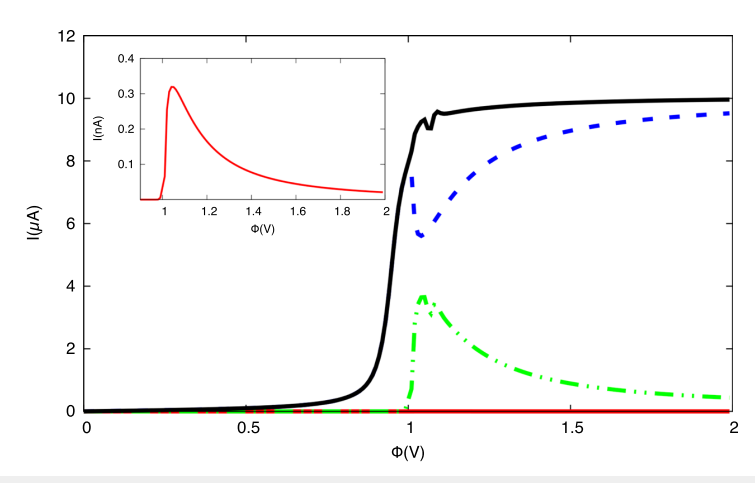


FIG. 7. Total steady-state current (black solid) is shown as a function of applied voltage in the molecular junction in addition to the coherent tunneling contributions from the neutral (blue dashed) and charged (green dotted-dashed) states. The inset shows the contributions of the hopping transport term from Eq. (50) (red solid). The coupling strength in this case was $\Gamma_R = \Gamma_L = 0.01035$ eV.

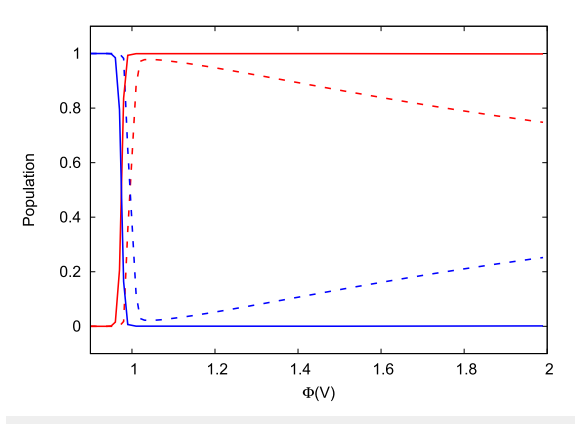


FIG. 8. Steady-state population for the neutral (blue) and charged (red) states as a function of applied bias for the asymmetric junction with $V_d^L/V_d^R=2$ (dashed) and 5 (solid). The case of $V_d^L/V_d^R=10$ lies on the same curves as the result for 5 and is not reproduced here.

only weakly physisorbed to the other.³⁸ The variation in the coupling strength is squared in the expressions for Γ_R and Γ_L , meaning that even small differences can lead to substantial changes in steady-state populations. From Fig. 4, it is clear that decreasing the right electrode coupling will significantly diminish the rate of electron transfer from the molecule in the charged state and should shift the steady-state populations. Figure 8 shows that nearly complete initial transfer of the population to the charged state is achieved in the case where the coupling to the left is twice that to the right electrode, followed by the same decline in charged state population with increasing bias voltage seen in Fig. 6. However, once the coupling differs by a factor of 5 or more, the population transfer is complete

and the molecule becomes fully charged once the molecular level is crossed by the left electrode Fermi level. In this case, the flow of population is decidedly one way and no further changes in steady-state distributions are seen after 1.0 V. Qualitatively, the scenario shown in Fig. 8 for the factor of 5 asymmetry resembles a redox event in which the molecule transitions from a neutral to charged state in a small bias voltage window and further demonstrates the potential of this ensemble scattering description to span both tunneling and redox processes in a consistent framework.

The current through the asymmetric junction is shown in Fig. 9 for the case where the left electrode coupling is five times greater than the coupling to the right. Clearly, the overall current is now less than it was for the symmetric case as a result of the smaller value for V_d^R . However, in the asymmetric case, there is also a significant drop in total current accompanied by the switch to the charged state. The drop in current can be rationalized based on the differences in the behavior of the transmission functions for the neutral and charged states discussed in Secs. III A and III B. In the case of transmission through the neutral state, we can see from Eq. (39) that the broadening of the molecular level will be dictated by the coupling to the right electrode since it is weighted by $[1 - f_R(\epsilon_l)]$ and the left electrode's contribution is eliminated by $[1 - f_L(\epsilon_l)]$. For tunneling through the charged state, Eq. (27) shows that the switch in Fermi functions changes the contributions from the left and right electrodes in comparison with the neutral state. For the charged states transmission, the contribution to the level width from the right electrode is eliminated since it is weighted by the Fermi function that will be evaluated at an energy above the right electrode Fermi level in Eq. (50). Thus, for the charged state transmission, the broadening arises solely from the left electrode. Since the coupling to the left electrode is stronger than the right in this asymmetric case, the broadening of the charged state is greater and a smaller and flatter transmission peak results. The net result is that the current through the charged state is suppressed relative to the neutral state, and once

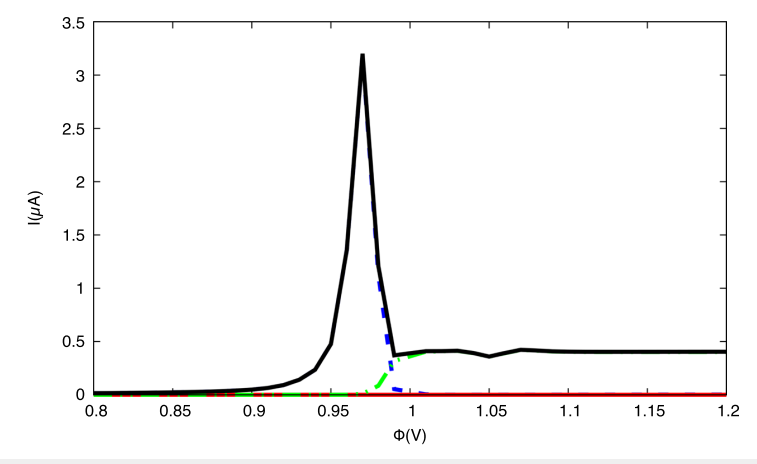


FIG. 9. Total steady-state current (black solid) is shown as a function of applied voltage in the molecular junction in addition to the coherent tunneling contributions from the neutral (blue dashed) and charged (green dotted-dashed) states. The contribution from the hopping term of Eq. (50) remains negligible (red solid), and the coupling strength in this case was $\Gamma_L = 25\Gamma_R = 0.01035$ eV.

an electron has attached itself to the molecule, the current is reduced. The drop in current with increasing voltage is an example of negative differential conductance, the presence of which has been ascribed to the onset of redox states in molecular junctions. ¹⁰² While the magnitude of the effect seen here is much smaller than reported from experiment, it is interesting that such an effect is recovered within our simple model and its appearance is tied closely to the inclusion of the many-electron nature of the electrodes via our treatment of the self-energy.

IV. CONCLUSION

In this work, we have introduced a novel generalized quantum master equation inspired by ensemble scattering theory to describe electron transfer in molecular junctions capable of spanning both the off-resonant tunneling regime and the on-resonant charging of the molecule. An important formal result from this investigation is the connection shown between the memory kernel and the Liouville transition and Møller superoperators. This framework forms a bridge between previous efforts focused on quantum master equations and scattering descriptions largely applied in two limiting regimes of charge transfer: coherent tunneling and sequential hopping. The important aspects of our generalized quantum master equation approach are its inclusion of all orders of electrode-molecule coupling, derivation of equations of motion for both Markovian and non-Markovian bath dynamics, inclusion of the many-electron nature of the electrodes via the voltage dependence of the self-energy expressions, and demonstrated connection to the Landauer picture in the appropriate limits. Regarding the final point, we have shown that the Landauer theory is recovered by invoking both the limit of elastic scattering and the binary collision approximation for the memory kernel in the master equation. The latter of these two points provides an interesting direction for future work in the development of approximate treatments for charge transport in molecular junctions that remain capable of spanning tunneling and hopping regimes. While this work has relied heavily on formal derivations, a simple one-site model was used to demonstrate the ability for the framework to capture the essential physics in the off-resonant and resonant transport regimes in the absence of vibrational coupling. There are many future directions to consider: the impact of the binary collision and Markovian approximations, the inclusion of vibrational effects on the current, and the role of interference from multiple charged states. We anticipate that this initial work will form the basis for continued development of novel master equations to describe charge transport in open quantum systems ranging from molecular junctions to electrochemical environments.

ACKNOWLEDGMENTS

This work was supported by funding from the Chemical Theory, Models, and Computation Methods program in the Division of Chemistry at the National Science Foundation (Grant No. CHE 1900423). Population dynamics calculations were performed on the Augie High-Performance Computing cluster at Villanova University, funded by the National Science Foundation, Award No. OAC 2018933.

AUTHOR DECLARATIONS

Conflict of Interest

The authors have no conflicts to disclose.

Author Contributions

David Bialas: Conceptualization (supporting); Data curation (lead); Formal analysis (equal); Software (lead); Writing – original draft (equal); Writing – review & editing (equal). Ryan Jorn: Conceptualization (lead); Formal analysis (lead); Project administration (lead).

DATA AVAILABILITY

The data that support the findings of this study are available from the corresponding author upon reasonable request.

APPENDIX A: THE NONINTERACTING ANDERSON HAMILTONIAN

Here, the explicit connection between the noninteracting Anderson model for charge transfer and the general Hamiltonian for a molecule attached between two electrode surfaces is clarified to emphasize the assumptions made along the way. It will be shown that the simplifications introduced in deriving expressions for the current and the evolution of the density matrix for a molecular junction in Sec. II flow from the same system—bath partitioning used to simplify the model Hamiltonian. In general, the molecule + electrodes system is described by

$$\begin{split} \hat{H} &= \frac{1}{2m_e} \sum_{i} \nabla_{r_i}^2 + \frac{1}{2} \sum_{i \neq j} \frac{1}{|\vec{r}_i - \vec{r}_j|} - \sum_{\substack{i \text{ leelectrodes} \\ I \in electrodes}} \frac{Z_I}{|\vec{r}_i - \vec{R}_I|} \\ &- \sum_{\substack{j \text{ emolecule} \\ J \in \text{molecule}}} \frac{Z_J}{|\vec{r}_i - \vec{R}_J|} + \sum_{\substack{I \text{ electrodes} \\ J \in \text{molecule}}} \frac{1}{2M_I} \nabla_{R_I}^2 \\ &+ \sum_{\substack{J \text{ emolecule} \\ J \in \text{molecule}}} \frac{1}{2M_J} \nabla_{R_J}^2 + \sum_{\substack{I \text{ electrodes} \\ J \in \text{molecule}}} \frac{Z_I Z_J}{|\vec{R}_I - \vec{R}_J|} \\ &+ \sum_{\substack{I,J' \text{ electrodes} \\ |\vec{R}_I - \vec{R}_{J'}|}} \frac{Z_I Z_{J'}}{|\vec{R}_I - \vec{R}_{J'}|} + \sum_{\substack{J,J' \text{ emolecule} \\ |\vec{R}_J - \vec{R}_{J'}|}} \frac{Z_J Z_{J'}}{|\vec{R}_J - \vec{R}_{J'}|}, \end{split} \tag{A1}$$

where atomic units are assumed and the electronic and nuclear indices are distinguished by lower-case and upper-case letters, respectively, with $Z_{I(j)}$ referring to the charge on the nucleus I(J), $\vec{r}_{i(j)}$ is the position vector for electron i(j), and $\vec{R}_{I(J)}$ is the position vector for nucleus I(J). In the spirit of the Born–Oppenheimer approximation, we can rewrite the Hamiltonian in the following form:

$$\begin{split} \hat{H} &= \hat{H}_{e}(\{R_{molec}\}, \{R_{elec}\}) + \sum_{I \in electrode} \frac{1}{2M_{I}} \nabla_{R_{I}}^{2} \\ &+ \sum_{J \in molecule} \frac{1}{2M_{J}} \nabla_{R_{J}}^{2} \sum_{\substack{I \in electrode \\ J \in molecule}} \frac{Z_{I}Z_{J}}{|\vec{R}_{I} - \vec{R}_{J}|} \\ &+ \sum_{I,J' \in electrodes} \frac{Z_{I}Z_{I'}}{|\vec{R}_{I} - \vec{R}_{I'}|} + \sum_{J,J' \in molecule} \frac{Z_{J}Z_{J'}}{|\vec{R}_{J} - \vec{R}_{J'}|}, \end{split}$$
(A2)

where the electronic Hamiltonian, \hat{H}_e , is defined by the first four terms in Eq. (A1) and depends parametrically on the nuclear coordinates of the molecule, $\{R_{molec}\}$, and the electrodes, $\{R_{elec}\}$. Given the electronic Hamiltonian, the basis set chosen to describe the adiabatic electronic wavefunction consists of atom-centered orbitals from two separate Fock equations: one for the bulk electrode unperturbed by the presence of the adsorbed molecule and the other for the molecular region neglecting the influence of the bulk electrode. In this system-bath type of partitioning, one can include the first several layers of the electrodes in the electronic structure calculation for the molecular region to incorporate a portion of the electrode non-perturbatively. 41,61 The influence of the remainder of the semiinfinite electrodes will be accounted for via the self-energy discussed in Sec. III. Following a Hartree-Fock treatment for the entire system, the electronic wavefunction is described by Slater determinants of the following form:89

$$|\xi_{\alpha}(\mathbf{x}_1)\xi_{\beta}(\mathbf{x}_2)\cdots\xi_{\omega}(\mathbf{x}_{N_e})\rangle,$$
 (A3)

where the coordinates of electron n are indicated by \mathbf{x}_n , there are a total of N_e electrons in the system, and the spin orbitals are given by the ξ functions, which are labeled with lower case Greek letters. The above state vector implies the normalized weighting of all possible permutations of the orbital indices among the electrons.

To account for charge transfer, Slater determinants are included for a reference neutral state and charge transferred states in which electrons have been removed from one orbital in the bulk electrodes and placed in a vacant orbital of the molecular region or vice versa. Starting with the neutral reference state energy, it can be shown that the various summations in Eq. (A1) can be divided to enforce the partitioning of the matrix element into contributions from the electrode and molecular subsystems,

$$\langle \xi_{\alpha} \xi_{\beta} \dots | \hat{H}_{e} | \xi_{\alpha} \xi_{\beta} \dots \rangle = \sum_{y \in electrodes} \epsilon_{\gamma} + \sum_{y' \in molecule} \epsilon_{\gamma'} - \frac{1}{2} \sum_{y, \zeta \in electrodes} \langle \xi_{y} \xi_{\zeta} | \frac{1}{|\vec{r}_{1} - \vec{r}_{2}|} | \xi_{y} \xi_{\zeta} \rangle + \frac{1}{2} \sum_{y, \zeta \in electrodes} \langle \xi_{y} \xi_{\zeta} | \frac{1}{|\vec{r}_{1} - \vec{r}_{2}|} | \xi_{\zeta} \xi_{y} \rangle$$

$$- \frac{1}{2} \sum_{y', \zeta \in molecule} \langle \xi_{y'} \xi_{\zeta} | \frac{1}{|\vec{r}_{1} - \vec{r}_{2}|} | \xi_{y'} \xi_{\zeta} \rangle + \frac{1}{2} \sum_{y', \zeta \in molecule} \langle \xi_{y'} \xi_{\zeta} | \frac{1}{|\vec{r}_{1} - \vec{r}_{2}|} | \xi_{\zeta} \xi_{y'} \rangle - \sum_{\substack{y \in electrodes \\ J \in molecule}} \langle \xi_{y} | \frac{Z_{J}}{|\vec{r}_{1} - \vec{R}_{J}|} | \xi_{y} \rangle$$

$$- \sum_{\substack{y' \in molecule \\ J \in electrodes}} \langle \xi_{y'} | \frac{Z_{J}}{|\vec{r}_{1} - \vec{R}_{J}|} | \xi_{y'} \rangle + \sum_{\substack{y' \in molecule \\ J \in electrodes}} \langle \xi_{y'} \xi_{\zeta} | \frac{1}{|\vec{r}_{1} - \vec{r}_{2}|} | \xi_{\zeta} \xi_{y'} \rangle - \sum_{\substack{y' \in molecule \\ J \in electrodes}} \langle \xi_{y'} \xi_{\zeta} | \frac{1}{|\vec{r}_{1} - \vec{r}_{2}|} | \xi_{\zeta} \xi_{y'} \rangle,$$
(A4)

where the summations over electrons in Eq. (A1) have been replaced by sums over occupied orbitals ascribed to either the bulk electrodes or molecular scattering regions according to the Hartree-Fock calculation from which they arise. The first two terms in Eq. (A4) are summations over Fock orbital energies that are corrected to give the total Hartree-Fock energies for the isolated subsystems. The correction terms, third through sixth in Eq. (A4), will be neglected subsequently because the focus in Sec. III will be on Green's operators, including differences in state energies. Hence, these terms for the neutral and singly charged states can be assumed comparable and not carried along explicitly. The last four terms on the right-hand side of Eq. (A4) correspond to the interaction between the charge distributions of the two separate subsystems: electron densities from orbitals in the electrode interacting with the nuclear charges in the molecule, the electron density on the molecule interacting with the nuclear charges of the electrode, and, finally, the Coulomb/exchange interaction between the electron clouds of the electrode and molecule individually. These types of interactions are similar to those used to describe dipole scattering of electrons from and have been shown to be negligible for inelastic currents in comparison with resonance scattering via molecular states. 106 Hence, the contribution of these mean-field interactions between the system and bath electrons will be ignored in crafting the Hamiltonian.

If the same set of spin orbitals are retained in both the ground and charge-transferred determinants, greatly simplified matrix elements can be derived for the energy of the charge-transferred states and their coupling to the ground state. The practice of reusing the same basis set of orbitals to describe the charge-transferred states is equivalent to Koopman's theorem and assumes that the occupied and unoccupied Fock orbitals from the ground state calculation do not deviate substantially when an extra electron is added to or subtracted from the molecule. While lacking in quantitative accuracy, such an assumption provides a useful starting point. The matrix elements describing the coupling between charge-transferred states are then given by

$$\begin{split} \left\langle \xi_{\alpha}\xi_{\beta} \dots \xi_{\nu'} \dots \middle| \hat{H}_{e} \middle| \xi_{\alpha}\xi_{\beta} \dots \xi_{\mu'} \dots \right\rangle \\ &= \left\langle \xi_{\nu'} \middle| \hat{F}_{molecule} \middle| \xi_{\mu'} \right\rangle - \sum_{I \in electrode} \left\langle \xi_{\nu'} \middle| \frac{Z_{I}}{|\vec{r}_{1} - \vec{R}_{I}|} \middle| \xi_{\mu'} \right\rangle \\ &+ \sum_{\gamma \in electrode} \left\langle \xi_{\nu'} \xi_{\gamma} \middle| \frac{1}{|\vec{r}_{1} - \vec{r}_{2}|} \middle| \xi_{\mu'} \xi_{\gamma} \right\rangle \\ &- \sum_{\gamma \in electrode} \left\langle \xi_{\nu'} \xi_{\gamma} \middle| \frac{1}{|\vec{r}_{1} - \vec{r}_{2}|} \middle| \xi_{\gamma} \xi_{\mu'} \right\rangle, \end{split} \tag{A5}$$

where the determinants differ by an electron exchanged between the orbitals $\xi_{\nu'}$ and $\xi_{\mu'}$ and $\hat{F}_{molecule}$ is the Fock operator for the molecule. Given that the orbitals involved in the exchange could come from either the electrodes or the adsorbate, there are three classes of matrix elements to consider for $\xi_{\nu'}$ and $\xi_{u'}$: both orbitals are in an electrode, both orbitals are on the molecule, or one orbital is localized on the electrode with the other on the molecule. Physically, the first two scenarios correspond to the same type of mean field charge-charge interactions discarded in the discussion of Eq. (A4) and will similarly be neglected here. The third class of transitions describe the charge exchange between the molecule and the electrodes, which is the process of fundamental interest to our discussion. Since the orbitals have been constructed from the Fock operators for the subsystems and can be orthogonalized with respect to each other, the first term in Eq. (A5) does not contribute to the coupling. One obtains an expression for a coupling operator connecting the neutral and charge-transferred states,

$$\begin{split} \left\langle \xi_{\alpha}\xi_{\beta}\dots\xi_{\gamma'}\dots \middle| \hat{H}^{e} \middle| \xi_{\alpha}\xi_{\beta}\dots\xi_{\mu'}\dots \right\rangle \\ &= \left\langle \xi_{\gamma'} \middle| \left(-\sum_{I e electrode} \frac{Z_{I}}{|\vec{r}_{1} - \vec{R}_{I}|} - \sum_{\gamma e electrode} \left\langle \xi_{\gamma} \middle| \frac{1}{|\vec{r}_{1} - \vec{r}_{2}|} \hat{P} \middle| \xi_{\gamma} \right\rangle \right. \\ &+ \sum_{\gamma e electrode} \left\langle \xi_{\gamma} \middle| \frac{1}{|\vec{r}_{1} - \vec{r}_{2}|} \middle| \xi_{\gamma} \right\rangle \left. \right) \middle| \xi_{\mu'} \right\rangle \\ &= V_{\gamma'\mu'}, \end{split} \tag{A6}$$

where the operator \hat{P} permutes the two orbitals on its right-hand side to give the correct exchange correlation. The common substitution of $V_{\nu'\mu'}$ has been used to describe the matrix element coupling orbitals $\xi_{\nu'}$ and $\xi_{\mu'}$ through an operator defined exclusively by the electrodes' electronic structure. Equation (A6) completes our goal of connecting the general Hamiltonian to the noninteracting Anderson model within Hartree–Fock theory,

$$\begin{split} \hat{H}_{e} &= \sum_{\gamma} \epsilon_{\gamma} (\{R_{elec}\}) \hat{c}_{\gamma}^{\dagger} c_{\gamma} + \sum_{d} \epsilon_{d} (\{R_{molec}\}) \hat{c}_{d}^{\dagger} c_{d} \\ &+ \sum_{\gamma d} V_{\gamma d} (\{R_{molec}\}, \{R_{elec}\}) (\hat{c}_{\gamma}^{\dagger} \hat{c}_{d} + \hat{c}_{d}^{\dagger} \hat{c}_{\gamma}), \end{split} \tag{A7}$$

where \hat{c} and \hat{c}^{\dagger} correspond to the annihilation and creation operators for the Fock orbitals, γ indicates an orbital from the electrodes, d corresponds to adsorbate orbitals, and the dependence of the orbital energies and couplings on nuclear coordinates is indicated in braces.

APPENDIX B: RELATING THE MEMORY KERNEL TO SCATTERING THEORY IN LIOUVILLE SPACE

Here, we shall demonstrate the validity of the superoperator product for the memory kernel introduced in Eq. (14) and the connection between the relevant superoperators and their Hilbert space counterparts used in Sec. II C. The detailed derivation of these results is appropriate given that our product form for the memory kernel makes a unique connection to the operators from scattering theory and the time-independent description of the Møller superoperator

is not readily found in the literature. We begin by introducing a projected Green's operator, $\hat{\mathcal{G}}_{Q}(\omega)$, as the Fourier transform of the projected evolution operator,

$$\theta(\tau)e^{-i\tau(\hat{\mathcal{I}}-\hat{\hat{V}}\,\hat{\mathcal{P}})} = \frac{i}{2\pi} \int_{-\infty}^{\infty} d\omega e^{-i\omega\tau} \frac{1}{\omega^{+} - \hat{\mathcal{L}} + \hat{\mathcal{V}}\hat{\mathcal{P}}}$$
$$= \frac{i}{2\pi} \int_{-\infty}^{\infty} d\omega e^{-i\omega\tau} \hat{\mathcal{G}}_{Q}(\omega^{+}), \tag{B1}$$

where $\theta(\tau)$ is the Heaviside function and the usual infinitesimal, " $+i\eta$," has been added to the frequency denoted by the "+" superscript.⁹⁷ The evaluation of the memory kernel in Eq. (12) becomes

$$\begin{split} \frac{d}{dt}\,\hat{\mathcal{P}}|W(t)\rangle\rangle &= -i\hat{\mathcal{P}}\,\hat{\mathcal{L}}_0\,\hat{\mathcal{P}}|W(t)\rangle\rangle - \frac{i}{2\pi}\int_0^t d\tau \\ &\times \int_{-\infty}^{\infty} d\omega\,\hat{\mathcal{P}}\,\hat{\mathcal{V}}\,\hat{\mathcal{Q}}\,\hat{\mathcal{G}}_Q(\omega)\,\hat{\mathcal{Q}}\,\hat{\mathcal{V}}\,\hat{\mathcal{P}}|W(t-\tau)\rangle\rangle, \quad (B2) \end{split}$$

which contains a frequency-dependent collection of operators reminiscent of the transition superoperator, except for the projection that remains onto the $\hat{\mathcal{Q}}$ subspace. In analogy to the description of the Hilbert space Green's operator, the projected Green's superoperator can be expanded as

$$\hat{\mathcal{G}}_{Q}(\omega^{+}) = \frac{1}{\omega^{+} - \hat{\mathcal{L}}} - \frac{1}{\omega^{+} - \hat{\mathcal{L}}} \hat{\mathcal{V}} \hat{\mathcal{P}} \frac{1}{\omega^{+} - \hat{\mathcal{L}} + \hat{\mathcal{V}} \hat{\mathcal{P}}}$$

$$= \hat{\mathcal{G}}(\omega^{+}) - \hat{\mathcal{G}}(\omega^{+}) \hat{\mathcal{V}} \hat{\mathcal{P}} \hat{\mathcal{G}}_{Q}(\omega^{+}), \tag{B3}$$

where the projection-free Green's superoperator, $\hat{\mathcal{G}}(\omega^+)$, has been introduced. Substituting this result into the expression for the memory kernel in Eq. (B2) yields an insightful expression as follows:

$$\hat{\bar{\mathcal{P}}}\hat{\mathcal{V}}\hat{\hat{\mathcal{Q}}}\hat{\hat{\mathcal{G}}}_Q(\omega^+)\,\hat{\hat{\mathcal{Q}}}\,\hat{\mathcal{V}}\hat{\bar{\mathcal{P}}}=\,\hat{\bar{\mathcal{P}}}\hat{\bar{\mathcal{T}}}(\omega^+)\,\hat{\bar{\mathcal{P}}}\Big(\hat{\bar{\mathcal{I}}}-\,\hat{\bar{\mathcal{P}}}\hat{\hat{\mathcal{G}}}_Q(\omega^+)\,\hat{\bar{\mathcal{Q}}}\,\hat{\mathcal{V}}\hat{\bar{\mathcal{P}}}\Big),\quad (B4)$$

where the memory kernel has been written in terms of the projection-free transition superoperator for the system–bath interaction [see Eq. (B8)] and a second term that acts as a correction to the projection-free result. As discussed in Sec. II B, dropping the projected Green's superoperator on the right-hand side of Eq. (B4) amounts to restricting the bath interactions to single collisions and ignores the possibility of multiple particle scattering events during a given interval of time. Hence, we view the term in parentheses in Eq. (B4) as a correction to the simple binary collision picture's to account for multiple sequential scattering events. With some additional work, it can be shown that the correction term can be connected to the Møller superoperator in Liouville space, $\hat{\Omega}(\omega) = \hat{\mathcal{I}} + \hat{\mathcal{G}}(\omega) \hat{\mathcal{V}}$,

$$\hat{\mathcal{P}}\hat{\mathcal{G}}_{Q}(\omega^{+})\hat{\mathcal{Q}}\hat{\mathcal{V}}\hat{\mathcal{P}} = \hat{\mathcal{P}}\hat{\Omega}(\omega^{+})\hat{\mathcal{P}} - \hat{\mathcal{P}} - \hat{\mathcal{P}}\hat{\mathcal{G}}(\omega^{+})\hat{\mathcal{V}}\hat{\mathcal{P}}\hat{\mathcal{G}}_{Q}(\omega^{+})\hat{\mathcal{Q}}\hat{\mathcal{V}}\hat{\mathcal{P}}$$

$$\hat{\Omega}(\omega^{+})\hat{\mathcal{P}}\hat{\mathcal{G}}_{Q}(\omega^{+})\hat{\mathcal{Q}}\hat{\mathcal{V}}\hat{\mathcal{P}} = \hat{\Omega}(\omega^{+})\hat{\mathcal{P}} - \hat{\mathcal{P}}.$$
(B5)

The derivation is completed by introducing the inverse of the Møller operator on both sides of Eq. (B5) to write the projected Green's operator as

$$\hat{\hat{\mathcal{P}}}\hat{\mathcal{G}}_{Q}(\omega^{+})\hat{\mathcal{Q}}\hat{\mathcal{V}}\hat{\mathcal{P}} = \hat{\mathcal{P}} - \hat{\mathcal{P}}\hat{\hat{\Omega}}^{-1}(\omega^{+})\hat{\mathcal{P}}.$$
 (B6)

Hence, we obtain our final compact result for the memory kernel,

$$\hat{\hat{\mathcal{P}}}\hat{\hat{\mathcal{V}}}\hat{\hat{\mathcal{Q}}}\hat{\hat{\mathcal{Q}}}_{O}(\omega^{+})\hat{\hat{\mathcal{Q}}}\hat{\hat{\mathcal{V}}}\hat{\hat{\mathcal{P}}} = \hat{\hat{\mathcal{P}}}\hat{\hat{\mathcal{T}}}(\omega^{+})\hat{\hat{\mathcal{P}}}\hat{\hat{\mathcal{P}}}\hat{\hat{\Omega}}^{-1}(\omega^{+})\hat{\hat{\mathcal{P}}}. \tag{B7}$$

It should be noted that in the special case that the frequencies chosen for the evaluation of the matrix element of the Møller superoperator are restricted to "on the frequency shell," the norm conversing property of the Møller operator (neglecting potential bound states) implies that the inverse is equal to the Hermitian conjugate, that is, $\hat{\Omega}^{-1}(\omega) = \hat{\Omega}^{\dagger}(\omega)$. In the case of the Markov limit discussed below, the memory kernel could then be written as a product of the transition superoperator and the conjugate of the Møller operator.

Having shown the relevance of the operators from Liouville space scattering theory, we conclude this section with the connection between the Liouville and Hilbert space representations. The form for $\hat{\mathcal{T}}$ was reported originally by Fano who leveraged the convolution representation for Green's superoperator. ¹⁰⁷ We revisit the highlights of this derivation here⁸⁶ as these expressions will prove useful in Sec. II D and demonstrate the means by which expressions for the Møller superoperator may be obtained. Consider a general matrix element of the superoperator,

$$\left\langle \left\langle C,D\right|\hat{\bar{\mathcal{T}}}(\omega)\big|A,B\right\rangle \right\rangle =\left\langle \left\langle C,D\right|\hat{\bar{\mathcal{V}}}\!|A,B\right\rangle \right\rangle +\left\langle \left\langle C,D\right|\hat{\bar{\mathcal{V}}}\!|\hat{\bar{\mathcal{G}}}(\omega)|\hat{\bar{\mathcal{V}}}\!|A,B\right\rangle \right\rangle ,$$

(B8

where the general indices A, B, C, D are used to indicate the states of \hat{H}_0 . Using the definitions for the action of the superoperators in terms of their Hilbert space counterparts, ⁹²

$$\begin{split} &\langle \langle C, D | \hat{\hat{\mathcal{V}}} | A, B \rangle \rangle = \langle C | \hat{\mathcal{V}} | A \rangle \delta_{DB} - \langle B | \hat{\mathcal{V}}^{\dagger} | D \rangle \delta_{AC} \\ &\langle \langle C, D | \hat{\hat{\mathcal{G}}}(\omega) | A, B \rangle \rangle = \frac{1}{2\pi i} \int_{-\infty}^{\infty} d\epsilon \langle C | \hat{G}(\epsilon + \omega) | A \rangle \langle B | \hat{G}^{\dagger}(\epsilon) | D \rangle, \end{split}$$

where δ_{AC} denotes the Kronecker delta between state labels A and C and the usual Hilbert space matrix elements are implied by the single bra–ket notation. After inserting the resolution of the identity between the operators in Eq. (B8), and with some additional rearrangement, one can find

$$\begin{split} \langle \langle C, D | \hat{\hat{T}}(\omega) | A, B \rangle \rangle \\ &= \langle C | \hat{V} | A \rangle \delta_{DB} - \langle B | \hat{V}^{\dagger} | D \rangle \delta_{AC} \\ &+ \frac{1}{2\pi i} \int_{-\infty}^{\infty} d\epsilon \langle C | \hat{V} \hat{G}(\epsilon + \omega) \hat{V} | A \rangle \langle B | \hat{G}^{\dagger}(\epsilon) | D \rangle \\ &- \frac{1}{2\pi i} \int_{-\infty}^{\infty} d\epsilon \langle C | \hat{G}(\epsilon + \omega) \hat{V} | A \rangle \langle B | \hat{G}^{\dagger}(\epsilon) \hat{V}^{\dagger} | D \rangle \\ &- \frac{1}{2\pi i} \int_{-\infty}^{\infty} d\epsilon \langle C | \hat{V} \hat{G}(\epsilon + \omega) | A \rangle \langle B | \hat{V}^{\dagger} \hat{G}^{\dagger}(\epsilon) | D \rangle \\ &+ \frac{1}{2\pi i} \int_{-\infty}^{\infty} d\epsilon \langle C | \hat{G}(\epsilon + \omega) | A \rangle \langle B | \hat{V}^{\dagger} \hat{G}^{\dagger}(\epsilon) \hat{V}^{\dagger} | D \rangle. \end{split}$$

$$(B10)$$

Using the Hilbert space equivalent to Eq. (B8) and the identities $\hat{G}(\epsilon)\hat{V} = \hat{G}_0(\epsilon)\hat{T}(\epsilon)$ and $\hat{V}\hat{G}(\epsilon) = \hat{T}(\epsilon)\hat{G}_0(\epsilon)$, one can show that the Liouville matrix element becomes

$$\langle \langle C, D | \hat{T}(\omega) | A, B \rangle \rangle$$

$$= \langle C | \hat{V} | A \rangle \delta_{DB} - \langle B | \hat{V}^{\dagger} | D \rangle \delta_{AC} + \frac{1}{2\pi i} \int_{-\infty}^{\infty} d\epsilon \langle C | \hat{T}(\epsilon + \omega) | A \rangle$$

$$\times \langle B | \hat{G}^{\dagger}(\epsilon) | D \rangle - \frac{1}{2\pi i} \int_{-\infty}^{\infty} d\epsilon \langle C | \hat{V} | A \rangle \langle B | \hat{G}^{\dagger}(\epsilon) | D \rangle$$

$$- \frac{1}{2\pi i} \int_{-\infty}^{\infty} d\epsilon \langle C | \hat{G}_{0}(\epsilon + \omega) \hat{T}(\epsilon + \omega) | A \rangle \langle B | \hat{G}_{0}^{\dagger}(\epsilon) \hat{T}^{\dagger}(\epsilon) | D \rangle$$

$$- \frac{1}{2\pi i} \int_{-\infty}^{\infty} d\epsilon \langle C | \hat{T}(\epsilon + \omega) \hat{G}_{0}(\epsilon + \omega) | A \rangle \langle B | \hat{T}^{\dagger}(\epsilon) \hat{G}_{0}^{\dagger}(\epsilon) | D \rangle$$

$$+ \frac{1}{2\pi i} \int_{-\infty}^{\infty} d\epsilon \langle C | \hat{G}(\epsilon + \omega) | A \rangle \langle B | \hat{T}^{\dagger}(\epsilon) | D \rangle$$

$$- \frac{1}{2\pi i} \int_{-\infty}^{\infty} d\epsilon \langle C | \hat{G}(\epsilon + \omega) | A \rangle \langle B | \hat{V}^{\dagger} | D \rangle. \tag{B11}$$

The integrals containing only Green's matrix elements as a function of energy can be replaced by the identity operator using the contour result ⁹⁷

$$\frac{1}{2\pi i} \int_{-\infty}^{\infty} d\epsilon \hat{G}^{\dagger}(\epsilon) = \hat{I}. \tag{B12}$$

Hence, these terms will cancel with the first two matrix elements of the scattering potential on the right-hand side of Eq. (B10),

$$\begin{split} \langle \langle C, D | \hat{\bar{T}}(\omega) | A, B \rangle \rangle &= \frac{1}{2\pi i} \int_{-\infty}^{\infty} d\epsilon \langle C | \hat{T}(\epsilon + \omega) | A \rangle \langle B | \hat{G}^{\dagger}(\epsilon) | D \rangle \\ &- \frac{1}{2\pi i} \int_{-\infty}^{\infty} d\epsilon \langle C | \hat{G}_{0}(\epsilon + \omega) \hat{T}(\epsilon + \omega) | A \rangle \\ &\times \langle B | \hat{G}_{0}^{\dagger}(\epsilon) \hat{T}^{\dagger}(\epsilon) | D \rangle - \frac{1}{2\pi i} \int_{-\infty}^{\infty} d\epsilon \\ &\times \langle C | \hat{T}(\epsilon + \omega) \hat{G}_{0}(\epsilon + \omega) | A \rangle \langle B | \hat{T}^{\dagger}(\epsilon) \hat{G}_{0}^{\dagger}(\epsilon) | D \rangle \\ &+ \frac{1}{2\pi i} \int_{-\infty}^{\infty} d\epsilon \langle C | \hat{G}(\epsilon + \omega) | A \rangle \langle B | \hat{T}^{\dagger}(\epsilon) | D \rangle. \end{split} \tag{B13}$$

Finally, the substitution for Green's operator in terms of \hat{T} allows us to write

$$\langle \langle C, D | \hat{T}(\omega) | A, B \rangle \rangle = \frac{1}{2\pi i} \int_{-\infty}^{\infty} d\epsilon \langle C | \hat{T}(\varepsilon + \omega) | A \rangle \langle B | \hat{G}_{0}^{\dagger}(\varepsilon) | D \rangle + \frac{1}{2\pi i} \int_{-\infty}^{\infty} d\epsilon \langle C | \hat{G}_{0}(\varepsilon + \omega) | A \rangle \langle B | \hat{T}^{\dagger}(\varepsilon) | D \rangle + \frac{1}{2\pi i} \int_{-\infty}^{\infty} d\epsilon \langle C | \hat{T}(\varepsilon + \omega) | A \rangle$$

$$\times \langle B | \hat{G}_{0}^{\dagger}(\varepsilon) \hat{T}^{\dagger}(\varepsilon) \hat{G}_{0}^{\dagger}(\varepsilon) | D \rangle - \frac{1}{2\pi i} \int_{-\infty}^{\infty} d\epsilon \langle C | \hat{G}_{0}(\varepsilon + \omega) \hat{T}(\varepsilon + \omega) | A \rangle \langle B | \hat{G}_{0}^{\dagger}(\varepsilon) \hat{T}^{\dagger}(\varepsilon) | D \rangle$$

$$- \frac{1}{2\pi i} \int_{-\infty}^{\infty} d\epsilon \langle C | \hat{T}(\varepsilon + \omega) \hat{G}_{0}(\varepsilon + \omega) | A \rangle \langle B | \hat{T}^{\dagger}(\varepsilon) \hat{G}_{0}^{\dagger}(\varepsilon) | D \rangle$$

$$+ \frac{1}{2\pi i} \int_{-\infty}^{\infty} d\epsilon \langle C | \hat{G}_{0}(\varepsilon + \omega) \hat{T}(\varepsilon + \omega) \hat{G}_{0}(\varepsilon + \omega) | A \rangle \langle B | \hat{T}^{\dagger}(\varepsilon) | D \rangle.$$
(B14)

This equation will provide a useful starting point for developing the expression for current, where the first two terms on the right-hand side can be rewritten using a generalized optical theorem (see Appendix D). The form quoted by Fano and Ben Reuven for the transition superoperator matrix element is found by using the following identity for the free Green's matrix and the transition operator with singularities in different half-planes: 86,107

$$\frac{1}{2\pi i} \int_{-\infty}^{\infty} d\epsilon \langle C|\hat{T}(\epsilon+\omega)|A\rangle \langle B|\hat{G}_{0}^{\dagger}(\epsilon)|D\rangle = \langle C|\hat{T}(E_{D}+\omega)|A\rangle \delta_{BD}.$$
(B15)

The result for the off-the-frequency shell Liouville element is then given by

$$\begin{split} \langle \langle C, D | \hat{T}(\omega) | A, B \rangle \rangle \\ &= \langle C | \hat{T}(E_D + \omega) | A \rangle \delta_{B,D} - \langle B | \hat{T}^{\dagger}(E_C - \omega) | D \rangle \delta_{A,C} \\ &+ \frac{1}{2\pi i} \lim_{\eta, \eta' \to 0} \int_{-\infty}^{\infty} d\epsilon \left[\frac{1}{\epsilon + \omega - E_C + i\eta} - \frac{1}{\epsilon - E_D - i\eta'} \right] \\ &\times \langle C | \hat{T}(\epsilon + \omega) | A \rangle \langle B | \hat{T}^{\dagger}(\epsilon) | D \rangle \\ &\times \left[\frac{1}{\epsilon + \omega - E_A + i\eta} - \frac{1}{\epsilon - E_B - i\eta'} \right]. \end{split} \tag{B16}$$

We shall also make use of the Markov limit for Eq. (B16) for which we take $\omega = \omega_{AB}$,

$$\langle \langle C, D | \hat{T}(\omega_{AB}) | A, B \rangle \rangle$$

$$= \langle C | \hat{T}(E_A) | A \rangle \delta_{B,D} - \langle B | \hat{T}^{\dagger}(E_B) | D \rangle \delta_{A,C}$$

$$- \lim_{\eta \to 0} \left[\frac{1}{E_A - E_C + i\eta} - \frac{1}{E_B - E_D - i\eta} \right]$$

$$\times \langle C | \hat{T}(E_A) | A \rangle \langle B | \hat{T}^{\dagger}(E_B) | D \rangle, \tag{B17}$$

Following a similar approach to that shown above for the transition superoperator, the expression for the Møller superoperator can also be derived using Green's superoperator convolution integral and the relationship $\hat{G}(\varepsilon) = \hat{G}_0(\varepsilon)\hat{\Omega}(\varepsilon)$,

$$\begin{split} \left\langle \left\langle C, D \middle| \hat{\bar{\Omega}}(\omega) \middle| A, B \right\rangle \right\rangle &= -\delta_{A,C} \delta_{B,D} + \frac{i}{2\pi} \lim_{\eta \to 0} \int_{-\infty}^{\infty} d\epsilon \left[\frac{1}{\epsilon + \omega - E_A + i\eta} \right. \\ &\left. - \frac{1}{\epsilon - E_B - i\eta'} \right] \left\langle C \middle| \hat{\Omega}(\epsilon + \omega) \middle| A \right\rangle \left\langle B \middle| \hat{\Omega}^{\dagger}(\epsilon) \middle| D \right\rangle. \end{split} \tag{B18}$$

With the Markov limit again given by evaluating the expression at ω_{AB} ,

$$\langle \langle C, D | \hat{\Omega}(\omega_{AB}) | A, B \rangle \rangle = -\delta_{A,C} \delta_{B,D} + \langle C | \hat{\Omega}(E_A) | A \rangle \langle B | \hat{\Omega}^{\dagger}(E_B) | D \rangle. \tag{B19}$$

APPENDIX C: DERIVATION OF THE SELF-ENERGY WITHIN THE SINGLE ACTIVE ELECTRON ANSATZ

Evaluating the self-energy term from Eq. (20), we obtain two sets of scattering interactions,

$$\begin{split} \hat{Q}\hat{V}_{SB}^{e-mole}\hat{P}\big(E^{+}-\hat{H}_{0}\big)^{-1}\hat{P}\hat{V}_{SB}^{e-mole}\hat{Q} &= \sum_{\substack{\{n_{\gamma}^{\prime\prime R}\},\{n_{\gamma}^{\prime\prime\prime L}\}\\d>\text{HOMO}}} \left[\sum_{j\in R^{*}}\hat{Q}\hat{V}_{SB}^{e-mole}\big|N,\{n_{\gamma}^{\prime\prime\prime R}+j\}\{n_{\gamma}^{\prime\prime\prime L}\}\big)\frac{\sqrt{n_{j}^{\prime\prime}+1}V_{jd}}{E^{+}-E_{N}-E_{\{n_{\gamma}^{\prime\prime\prime R}\}\{n_{\gamma}^{\prime\prime\prime L}\}-\epsilon_{j}}}\right] \\ &+ \sum_{l\in L^{*}}\hat{Q}\hat{V}_{SB}^{e-mole}\big|N,\{n_{\gamma}^{\prime\prime\prime R}\}\{n_{\gamma^{\prime\prime}}^{\prime\prime\prime L}+l\}\big)\frac{\sqrt{n_{j}^{\prime\prime\prime}+1}V_{ld}}{E^{+}-E_{N}-E_{\{n_{\gamma}^{\prime\prime\prime R}\}\{n_{\gamma}^{\prime\prime\prime L}\}-\epsilon_{j}}}\bigg] \Big\langle N+d,\{n_{\gamma}^{\prime\prime\prime R}\}\{n_{\gamma^{\prime\prime}}^{\prime\prime\prime L}\}\big| \end{split}$$

$$+ \sum_{\substack{\{n_{j''}^{\prime\prime\prime R}\}, \{n_{j''}^{\prime\prime\prime L}\}\\d \leq \text{HOMO}}} \left[\sum_{j \in R^{**}} \hat{Q} \hat{V}_{SB}^{e-mole} \middle| N, \{n_{j'}^{\prime\prime\prime R} - j\} \{n_{j'}^{\prime\prime L}\} \right) \frac{\sqrt{n_{j'}^{\prime\prime}} \hat{V}_{jd}}{E^{+} - E_{N} - E_{\{n_{j''}^{\prime\prime\prime R}\}} \{n_{j''}^{\prime\prime\prime L}\} + \epsilon_{j}}$$

$$+ \sum_{\substack{l \in L^{**}\\H_{N}}} \hat{Q} \hat{V}_{SB}^{e-mole} \middle| N, \{n_{j'}^{\prime\prime\prime R}\} \{n_{j'}^{\prime\prime\prime L} - l\} \right) \frac{\sqrt{n_{j'}^{\prime\prime}} V_{ld}}{E^{+} - E_{N} - E_{\{n_{j'}^{\prime\prime\prime R}\}} \{n_{j'}^{\prime\prime\prime L}\} + \epsilon_{l}} \left[\langle N - d, \{n_{j'}^{\prime\prime\prime R}\} \{n_{j'}^{\prime\prime\prime L}\} \middle|, \right]$$

$$(C1)$$

where the first two terms correspond to the anion of the molecule donating an electron to the electrodes and the second set of terms show the cation taking on a charge from either electrode. The form for the electronic coupling, see Eq. (4), restricts the allowed transitions to electrode configurations that differ by one electron. Furthermore, Pauli exclusion restricts transitions between electrode configurations to orbitals that are either originally vacant (denoted by * in the first two terms) or previously occupied (denoted by ** in the second set of terms) for electron donation and removal, respectively. The sums over the electrode orbitals j and l correspond to the right and left electrode orbitals, and the occupation numbers for the orbitals also appear due to the action of the respective creation/annihilation operator.

The application of the second electron scattering interaction in all four terms of Eq. (C1) connects each initial anion and cation state with all possible singly charged states of the molecule and generates several new electrode configurations. Recall that multiply charged states have been excluded by our choice of the projection operators and system Hamiltonian in Sec. II A. With respect to

the electrode configurations, the second scattering interaction connects the initial state with configurations that have been altered by up to two orbital occupations. For example, application of the second scattering potential to the first term in Eq. (C1) produces electrode configurations described by $N + d', \{n_{\gamma}^{\prime\prime R} + j - j'\}\{n_{\gamma'}^{\prime\prime L}\}$ and $N - d', \{n_{\gamma}^{"R} + j + j'\}\{n_{\gamma'}^{"L}\}\$. Contrasting these possibilities with the incoming scattering state characterized by \hat{P} reveals that these matrix elements require the correlated movement of two electrons between the electrode and molecular subsystem: in general, one electron has been added/removed from the molecular subspace and a second electron has also been displaced from its original orbital. In the context of previous electron scattering treatments, these terms are excluded by the focus on a single electron event and will be dropped from our current discussion in favor of a "single active electron" (SAE) Ansatz for the self-energy. It can be shown that this *Ansatz* is equivalent to the requirement that the selfenergy be diagonal with respect to the electrode configuration and decouples the different charged states of the system,

$$\begin{split} \hat{Q}\hat{V}_{SB}^{e-mole}\hat{P}\left(E^{+}-\hat{H}_{0}\right)^{-1}\hat{P}\hat{V}_{SB}^{e-mole}\hat{Q} &\overset{\text{SAE}}{\Longrightarrow} \sum_{\substack{\{n_{\gamma}^{\prime\prime\prime}\},\{n_{\gamma}^{\prime\prime\prime}\}\\d,d'>\text{HOMO}}} \left|N+d',\{n_{\gamma}^{\prime\prime\prime}\}\{n_{\gamma'}^{\prime\prime\prime}\}\right| \sum_{j\in\mathbb{R}^{*}} \frac{(n_{j}^{\prime\prime}+1)V_{jd'}V_{jd}}{E^{+}-E_{N}-E_{\{n_{\gamma}^{\prime\prime\prime}\}}\{n_{\gamma'}^{\prime\prime\prime}\}-\epsilon_{j}} \\ &+\sum_{l\in\mathbb{L}^{*}} \frac{(n_{l}^{\prime\prime}+1)V_{ld'}V_{ld}}{E^{+}-E_{N}-E_{\{n_{\gamma}^{\prime\prime\prime}\}}\{n_{\gamma'}^{\prime\prime\prime}\}-\epsilon_{l}} \right] \left\langle N+d,\{n_{\gamma}^{\prime\prime\prime}\}\{n_{\gamma'}^{\prime\prime\prime}\}\right| + \sum_{\substack{\{n_{\gamma}^{\prime\prime\prime}\},\{n_{\gamma'}^{\prime\prime\prime}\}\\d,d'\leq\text{HOMO}}} \left|N-d',\{n_{\gamma}^{\prime\prime\prime}\}\{n_{\gamma'}^{\prime\prime\prime}\}\right| \\ &\times\left[\sum_{j\in\mathbb{R}^{**}} \frac{n_{j}^{\prime\prime}V_{jd'}V_{jd}}{E^{+}-E_{N}-E_{\{n_{\gamma}^{\prime\prime\prime}\}}\{n_{\gamma'}^{\prime\prime\prime}\}+\epsilon_{j}} + \sum_{l\in\mathbb{L}^{**}} \frac{n_{l}^{\prime\prime\prime}V_{ld'}V_{ld}}{E^{+}-E_{N}-E_{\{n_{\gamma}^{\prime\prime\prime}\}}\{n_{\gamma'}^{\prime\prime\prime}\}+\epsilon_{l}} \right] \left\langle N-d,\{n_{\gamma}^{\prime\prime\prime\prime}\}\{n_{\gamma'}^{\prime\prime\prime}\}\right|. \end{aligned} \tag{C2}$$

The same line of argument can be used for simplifying the self-energy arising from incoming charged states present in Eq. (25). One can show that, similar to Eq. (C1), the electrode configuration can be changed by the addition/subtraction of electrons from the available orbitals as the molecule transitions from the neutral state to a charged state [in the opposite order of Eq. (C1)] and that the assumption of a diagonal self-energy in the electrode configuration amounts to neglecting the motion of additional electrons during the scattering event. The difference between evaluating Eqs. (20) and (25) comes from the difference in the incoming states and the Pauli exclusion restrictions on the relevant sums,

$$\begin{split} \hat{P} \hat{V}_{SB}^{e-mole} \hat{Q} \Big(E^{+} - \hat{H}_{0} \Big)^{-1} \hat{Q} \hat{V}_{SB}^{e-mole} \hat{P} & \xrightarrow{\sum_{\{n_{\gamma}^{\prime\prime\prime R}\}, \{n_{\gamma^{\prime\prime}}^{\prime\prime\prime L}\}}} \left| N, \{n_{\gamma}^{\prime\prime R}\} \{n_{\gamma^{\prime\prime}}^{\prime\prime L}\} \right\rangle \\ & = \sum_{\substack{j \in R^{**} \\ d > \text{HOMO}}} \frac{(n_{j}^{\prime\prime}) V_{jd} V_{jd}}{E^{+} - E_{N} - \epsilon_{d} - E_{\{n_{\gamma}^{\prime\prime\prime R}\} \{n_{\gamma^{\prime\prime}}^{\prime\prime\prime L}\} + \epsilon_{j}}} \\ & + \sum_{\substack{l \in L^{**} \\ d > \text{HOMO}}} \frac{(n_{j}^{\prime\prime\prime}) V_{ld} V_{ld}}{E^{+} - E_{N} - \epsilon_{d} - E_{\{n_{\gamma}^{\prime\prime\prime R}\} \{n_{\gamma^{\prime\prime}}^{\prime\prime\prime L}\} + \epsilon_{l}}} \right] \left\langle N, \{n_{\gamma}^{\prime\prime\prime R}\} \{n_{\gamma^{\prime\prime}}^{\prime\prime\prime L}\} \right| \end{split}$$

$$+ \sum_{\substack{\{n_{j'}^{\prime\prime R}\}, \{n_{j'}^{\prime\prime\prime I}\}\\ d \leq \text{HOMO}}} \left| N, \{n_{j'}^{\prime\prime\prime R}\} \{n_{j'}^{\prime\prime\prime L}\} \right\rangle \left[\sum_{\substack{j \in R^{*}\\ d \leq \text{HOMO}}} \frac{(n_{j}^{\prime\prime} + 1) V_{jd} V_{jd}}{E^{+} - E_{N} + \epsilon_{d} - E_{\{n_{j'}^{\prime\prime\prime R}\} \{n_{j'}^{\prime\prime\prime L}\} - \epsilon_{j}}} \right] \\ + \sum_{\substack{l \in L^{*}\\ d \leq \text{HOMO}}} \frac{(n_{l}^{\prime\prime\prime} + 1) V_{ld} V_{ld}}{E^{+} - E_{N} + \epsilon_{d} - E_{\{n_{j''}^{\prime\prime\prime R}\} \{n_{j'}^{\prime\prime\prime L}\} - \epsilon_{l}}} \left| \langle N, \{n_{j'}^{\prime\prime\prime R}\} \{n_{j'}^{\prime\prime\prime L}\} |, \right.$$
(C3)

where the same notation appears as in Eq. (C2), where ** denotes a restriction on the summation to orbitals that are originally occupied and * denotes a restriction on the summation to unoccupied electrode orbitals that can accept an electron from the molecule.

APPENDIX D: A GENERALIZED OPTICAL THEOREM FOR THE CURRENT EXPRESSION

While the optical theorem is an important relationship in scattering descriptions, 108 a slightly generalized version is required in the discussion of Sec. II D to obtain the desired form for the current. It can be shown that proving the norm conservation of Eqs. (14) and (15) also relies on this generalized optical theorem to connect the first two integrals in Eq. (B14) to the remaining four. We motivate our form for the optical theorem following the derivation presented by Levine 97 and start with the expansion for the transition operator in Hilbert space,

$$\hat{T}(E^{+}) = \hat{V} + \hat{V}\hat{G}_{0}(E^{+})T(E^{+}),$$
 (D1)

where \hat{V} is the scattering potential, \hat{G}_0 is the free Green's operator, and E^+ corresponds to the appropriate incoming energy state with the boundary condition designated by "+." If we consider the evaluation of the transition operator at two different energies, E_A and E_B , it can be seen that

$$\begin{split} \left[\hat{I} + \hat{G}_{0}(E_{B}^{+}) \hat{T}(E_{B}^{+}) \right]^{\dagger} \hat{V} \left[\hat{I} + \hat{G}_{0}(E_{A}^{+}) \hat{T}(E_{A}^{+}) \right] \\ &= \hat{T}^{\dagger} (E_{B}^{+}) \left[\hat{I} + \hat{G}_{0}(E_{A}^{+}) \hat{T}(E_{A}^{+}) \right] \\ &= \left[\hat{I} + \hat{G}_{0}(E_{B}^{+}) \hat{T}(E_{B}^{+}) \right]^{\dagger} \hat{T}(E_{A}^{+}), \end{split} \tag{D2}$$

where the scattering potential is assumed to be real valued such that $\hat{V}^{\dagger}=\hat{V}.$ From the above, it follows that

$$\hat{T}(E_A^+) - \hat{T}^{\dagger}(E_B^+) = \hat{T}^{\dagger}(E_B^+) \Big[\hat{G}_0(E_A^+) - \hat{G}_0^{\dagger}(E_B^+) \Big] \hat{T}(E_A^+). \tag{D3}$$

In the context of the current expression, the first two terms in Eq. (B14) contribute the following to Eq. (32):

$$\begin{split} &\sum_{\{n_{\gamma}^{R}\}\{n_{\gamma'}^{L}\}} \sum_{\{n_{\gamma'}^{R}\}\{n_{\gamma'}^{L}\}} \left(\sum_{\gamma' \in L} n_{\gamma'}^{L} \right) P_{\{n_{\gamma'}^{R}\}} P_{\{n_{\gamma'}^{L}\}} \\ &\times \sum_{M,M',M''} \left\{ \int_{-\infty}^{\infty} d\epsilon \left\langle M\{n_{\gamma}^{R}\}\{n_{\gamma'}^{L}\} \middle| \hat{T}(\epsilon + \omega) \middle| M'\{n_{\gamma'}^{R}\}\{n_{\gamma'}^{L}\} \right\rangle \right. \\ &\times \left\langle M''\{n_{\gamma'}^{R}\}\{n_{\gamma'}^{L}\} \middle| \hat{G}_{0}^{\dagger}(\epsilon) \middle| M\{n_{\gamma}^{R}\}\{n_{\gamma'}^{L}\} \right\rangle \\ &+ \int_{-\infty}^{\infty} d\epsilon \left\langle M\{n_{\gamma}^{R}\}\{n_{\gamma'}^{L}\} \middle| \hat{G}_{0}(\epsilon + \omega) \middle| M'\{n_{\gamma'}^{R}\}\{n_{\gamma'}^{L}\} \right\rangle \\ &\times \left\langle M''\{n_{\gamma'}^{R}\}\{n_{\gamma'}^{L}\} \middle| \hat{T}^{\dagger}(\epsilon) \middle| M\{n_{\gamma}^{R}\}\{n_{\gamma'}^{L}\} \right\rangle \left. \left\langle (M',M''), \right. \end{split} \tag{D4}$$

where the indices follow the nomenclature used throughout this work, e.g., M denotes the states of the molecular subsystem and the electrode configurations are noted by the $\{n^{RL}\}$ indices. We can eliminate summations by recognizing that the free Green's operator is diagonal in state space and performing some minor rearrangement.

$$= \sum_{\{n_{\gamma}^{R}\}\{n_{\gamma'}^{L}\}} \left(\sum_{\gamma' \in L} n_{\gamma'}^{L} \right) P_{\{n_{\gamma}^{R}\}} P_{\{n_{\gamma'}^{L}\}} \sum_{M',M''} \left\{ \int_{-\infty}^{\infty} d\epsilon \right. \\ \left. \times \left\langle M'' \{n_{\gamma}^{R}\}\{n_{\gamma'}^{L}\} \middle| \left[\hat{G}_{0}^{\dagger}(\epsilon) \hat{T}(\epsilon + \omega) + \hat{T}^{\dagger}(\epsilon) \hat{G}_{0}(\epsilon + \omega) \right] \right. \\ \left. \times \left| M' \{n_{\gamma}^{R}\}\{n_{\gamma'}^{L}\} \right\} \right\} \langle \langle M', M'' |.$$
 (D5)

The key step is now to make use of the relationship in Eq. (D3) between the transition operator and its conjugate when combined with the respective free Green's operator,

$$= \sum_{\{n_{\gamma}^{R}\}\{n_{\gamma'}^{L}\}} \left\{ \sum_{\gamma'\in L} n_{\gamma'}^{L} \right\} P_{\{n_{\gamma'}^{R}\}} P_{\{n_{\gamma'}^{L}\}} \sum_{M',M''} \left\{ -\int_{-\infty}^{\infty} d\epsilon \left\langle M''\{n_{\gamma}^{R}\}\{n_{\gamma'}^{L}\} | \hat{G}_{0}^{\dagger}(\epsilon) \hat{T}^{\dagger}(\epsilon) \hat{G}_{0}^{\dagger}(\epsilon) \hat{T}(\epsilon+\omega) | M'\{n_{\gamma}^{R}\}\{n_{\gamma'}^{L}\} \right\} \right. \\ \left. + \int_{-\infty}^{\infty} d\epsilon \left\langle M''\{n_{\gamma}^{R}\}\{n_{\gamma'}^{L}\} | \hat{G}_{0}^{\dagger}(\epsilon) \hat{T}^{\dagger}(\epsilon) \hat{G}_{0}(\epsilon+\omega) \hat{T}(\epsilon+\omega) | M'\{n_{\gamma}^{R}\}\{n_{\gamma'}^{L}\} \right) + \int_{-\infty}^{\infty} d\epsilon \left\langle M''\{n_{\gamma}^{R}\}\{n_{\gamma'}^{L}\} | \hat{G}_{0}^{\dagger}(\epsilon) \hat{T}^{\dagger}(\epsilon) | M'\{n_{\gamma}^{R}\}\{n_{\gamma'}^{L}\} \right) \right. \\ \left. + \int_{-\infty}^{\infty} d\epsilon \left\langle M''\{n_{\gamma}^{R}\}\{n_{\gamma'}^{L}\} | \hat{T}(\epsilon+\omega) \hat{G}_{0}(\epsilon+\omega) | M'\{n_{\gamma}^{R}\}\{n_{\gamma'}^{L}\} \right) + \int_{-\infty}^{\infty} d\epsilon \left\langle M''\{n_{\gamma}^{R}\}\{n_{\gamma'}^{L}\} | \hat{T}^{\dagger}(\epsilon) \hat{G}_{0}(\epsilon+\omega) | M'\{n_{\gamma}^{R}\}\{n_{\gamma'}^{L}\} \right) \\ \left. - \int_{-\infty}^{\infty} d\epsilon \left\langle M''\{n_{\gamma}^{R}\}\{n_{\gamma'}^{L}\} | \hat{T}^{\dagger}(\epsilon) \hat{G}_{0}(\epsilon+\omega) \hat{T}(\epsilon+\omega) \hat{G}_{0}(\epsilon+\omega) | M'\{n_{\gamma}^{R}\}\{n_{\gamma'}^{L}\} \right) \right\} \left. \langle \langle M', M''|. \right. \tag{D6}$$

Using the same relationships from Appendix B, one can show that the third and fourth integrals evaluate to zero. In specific, the product of the free Green's operator and the transition operator evaluated at the same energy can be replaced by $\hat{V}\hat{G}(\epsilon + \omega)$, or the equiv-

alent expression for the conjugates, and one is left with integrals over Green's operator, which reduce to the identity and cancel one another. We are then left with the result that Eq. (D4) can be replaced

$$\begin{split} &= \sum_{\{n_{\gamma}^{R}\}\{n_{\gamma'}^{L}\}} \left(\sum_{\gamma'\in L} n_{\gamma'}^{L} \right) P_{\{n_{\gamma}^{R}\}} P_{\{n_{\gamma'}^{L}\}} \sum_{M',M''} \left\{ - \int_{-\infty}^{\infty} d\epsilon \left\langle M''\{n_{\gamma}^{R}\}\{n_{\gamma'}^{L}\} \middle| \hat{G}_{0}^{\dagger}(\epsilon) \hat{T}^{\dagger}(\epsilon) \hat{G}_{0}^{\dagger}(\epsilon) \hat{T}(\epsilon + \omega) \middle| M'\{n_{\gamma}^{R}\}\{n_{\gamma'}^{L}\} \right\rangle \right. \\ &+ \int_{-\infty}^{\infty} d\epsilon \left\langle M''\{n_{\gamma}^{R}\}\{n_{\gamma'}^{L}\} \middle| \hat{G}_{0}^{\dagger}(\epsilon) \hat{T}^{\dagger}(\epsilon) \hat{G}_{0}(\epsilon + \omega) \hat{T}(\epsilon + \omega) \middle| M'\{n_{\gamma}^{R}\}\{n_{\gamma'}^{L}\} \right\rangle \\ &+ \int_{-\infty}^{\infty} d\epsilon \left\langle M''\{n_{\gamma}^{R}\}\{n_{\gamma'}^{L}\} \middle| \hat{T}^{\dagger}(\epsilon) \hat{G}_{0}^{\dagger}(\epsilon) \hat{T}(\epsilon + \omega) \hat{G}_{0}(\epsilon + \omega) \middle| M'\{n_{\gamma}^{R}\}\{n_{\gamma'}^{L}\} \right\rangle \\ &- \int_{-\infty}^{\infty} d\epsilon \left\langle M''\{n_{\gamma}^{R}\}\{n_{\gamma'}^{L}\} \middle| \hat{T}^{\dagger}(\epsilon) \hat{G}_{0}(\epsilon + \omega) \hat{T}(\epsilon + \omega) \hat{G}_{0}(\epsilon + \omega) \middle| M'\{n_{\gamma}^{R}\}\{n_{\gamma'}^{L}\} \right\rangle \left. \left\langle \langle M', M'' \rangle \right. \end{split} \tag{D7}$$

Changing the labels on the electrode configurations by swapping $\{n_{\nu}^{R}\}\$ for $\{n_{\nu}^{\prime R}\}\$, we can now see that the contribution from the first two integrals in Eq. (B14) will look very similar to the remaining four integrals from Eq. (B14) that contribute to the current. The only difference will be that they are opposite in sign and contain a sum over the orbital occupations in the primed electrode configuration (the initial configuration operated on in the transition matrix element) rather than the sum over occupations in the final electrode configuration after the scattering event. Hence, we obtain the difference formula for current shown in Sec. II D.

REFERENCES

¹K. Leung, "Electronic structure modeling of electrochemical reactions at electrode/electrolyte interfaces in lithium ion batteries," J. Phys. Chem. C 117, 1539-1547 (2013).

²M. Gauthier, T. J. Carney, A. Grimaud, L. Giordano, N. Pour, H.-H. Chang, D. P. Fenning, S. F. Lux, O. Paschos, C. Bauer, F. Maglia, S. Lupart, P. Lamp, and Y. Shao-Horn, "Electrode-electrolyte interface in Li-ion batteries: Current understanding and new insights," J. Phys. Chem. Lett. 6, 4653-4672 (2015).

³L. Hammarström and S. Styring, "Coupled electron transfers in artificial photosynthesis," Philos. Trans. R. Soc., B 363, 1283-1291 (2008).

⁴M. D. Kärkäs, E. V. Johnston, O. Verho, and B. Åkermark, "Artificial photosynthesis: From nanosecond electron transfer to catalytic water oxidation," Acc. Chem. Res. 47, 100-111 (2014).

⁵X.-K. Chen, V. Coropceanu, and J. L. Brédas, "Assessing the nature of the charge-transfer electronic states in organic solar cells," Nat. Commun. 9, 5295

⁶E. C. P. Smits, T. D. Anthopoulos, S. Setayesh, E. van Veenendaal, R. Coehoorn, P. W. M. Blom, B. de Boer, and D. M. de Leeuw, "Ambipolar charge transport in organic field-effect transistors," Phys. Rev. B 73, 205316 (2006)

⁷V. May and O. Kühn, Charge and Energy Transfer Dynamics in Molecular Systems, 3rd ed. (Wiley, Weinheim, Germany, 2011).

 $^{\bf 8}{\rm R.\,A.\,Marcus},$ "On the theory of oxidation-reduction reactions involving electron transfer. I," J. Chem. Phys. 24, 966-978 (1956).

⁹ H. Imahori, K. Tamaki, D. M. Guldi, C. Luo, M. Fujitsuka, O. Ito, Y. Sakata, and S. Fukuzumi, "Modulating charge separation and charge recombination dynamics in porphyrin-fullerene linked dyads and triads: Marcus-normal versus inverted region," J. Am. Chem. Soc. 123, 2607-2617 (2001).

¹⁰A. Koch, D. Kinzel, F. Dröge, S. Gräfe, and S. Kupfer, "Photochemistry and electron transfer kinetics in a photocatalyst model assessed by Marcus theory and quantum dynamics," J. Phys. Chem. C 121, 16066–16078 (2017).

11 P. Song, Y. Li, F. Ma, T. Pullerits, and M. Sun, "Photoinduced electron transfer

in organic solar cells," Chem. Rec. 16, 734-753 (2016).

¹²Y. Li, Y. Feng, and M. Sun, "Photoinduced charge transport in a BHJ solar cell controlled by an external electric field," Sci. Rep. 5, 13970 (2015).

¹³ M.-L. Tan, E. A. Dolan, and T. Ichiye, "Understanding intramolecular electron transfer in ferredoxin: A molecular dynamics study," J. Phys. Chem. B 108, 20435-20441 (2004).

¹⁴A. Laurynėnas, M. Butkevičius, M. Dagys, S. Shleev, and J. Kulys, "Consecutive Marcus electron and proton transfer in heme peroxidase compound II-catalysed oxidation revealed by Arrhenius plots," Sci. Rep. 9, 14092 (2019).

¹⁵L. Yuan, L. Wang, A. R. Garrigues, L. Jiang, H. V. Annadata, M. Anguera Antonana, E. Barco, and C. A. Nijhuis, "Transition from direct to inverted charge transport Marcus regions in molecular junctions via molecular orbital gating, at. Nanotechnol. 13, 322-329 (2018).

16 B. Han, Y. Li, X. Ji, X. Song, S. Ding, B. Li, H. Khalid, Y. Zhang, X. Xu, L. Tian, H. Dong, X. Yu, and W. Hu, "Systematic modulation of charge transport in molecular devices through facile control of molecule-electrode coupling using a double selfassembled monolayer nanowire junction," J. Am. Chem. Soc. 142, 9708 (2020).

¹⁷J. O. Thomas, B. Limburg, J. K. Sowa, K. Willick, J. Baugh, G. A. D. Briggs, E. M. Gauger, H. L. Anderson, and J. A. Mol, "Understanding resonant charge transport through weakly coupled single-molecule junctions," Nat. Commun. 10,

¹⁸ A. Migliore, P. Schiff, and A. Nitzan, "On the relationship between molecular state and single electron pictures in simple electrochemical junctions," Phys. m. Chem. Phys. 14, 13746 (2012).

¹⁹A. Migliore and A. Nitzan, "Irreversibility and hysteresis in redox molecular conduction junctions," J. Am. Chem. Soc. 135, 9420-9432 (2013).

²⁰H. Kirchberg and A. Nitzan, "Energy transfer and thermoelectricity in molecular junctions in non-equilibrated solvents," J. Chem. Phys. 156, 094306 (2022);

 $^{\mathbf{21}}$ R. Landauer, "Spatial variation of currents and fields due to localized scatterers in metallic conduction," IBM J. Res. Dev. 1, 223-231 (1957)

²²M. Büttiker and R. Landauer, "Traversal time for tunneling," Phys. Rev. Lett. 49, 1739-1742 (1982).

²³ M. Čížek, M. Thoss, and W. Domcke, "Theory of vibrationally inelastic electron transport through molecular bridges," Phys. Rev. B 70, 125406 (2004).

²⁴Y. Meir and N. S. Wingreen, "Landauer formula for the current through an interacting electron region," Phys. Rev. Lett. 68, 2512-2515 (1992).

- 25 B. C. Stipe, M. A. Rezaei, and W. Ho, "Single-molecule vibrational spectroscopy and microscopy," Science 280, 1732-1735 (1998).
- ²⁶ A. N. Pasupathy, J. Park, C. Chang, A. V. Soldatov, S. Lebedkin, R. C. Bialczak, J. E. Grose, L. A. K. Donev, J. P. Sethna, D. C. Ralph, and P. L. McEuen, "Vibration-assisted electron tunneling in C₁₄₀ transistors," Nano Lett. 5, 203–207 (2005).
- ²⁷C.-l. Chiang, C. Xu, Z. Han, and W. Ho, "Real-space imaging of molecular structure and chemical bonding by single-molecule inelastic tunneling probe," Sci 344, 885-888 (2014).
- ²⁸S. Du, Y. Hashikawa, H. Ito, K. Hashimoto, Y. Murata, Y. Hirayama, and K. Hirakawa, "Inelastic electron transport and ortho-para fluctuation of water molecule in H₂O@C₆₀ single molecule transistors," Nano Lett. 21, 10346-10353
- (2021).

 29 M. Galperin, M. A. Ratner, and A. Nitzan, "Molecular transport junctions: Vibrational effects," J. Phys.: Condens. Matter 19, 103201 (2007).
- ³⁰ M. A. Reed, "Inelastic electron tunneling spectroscopy," Mater. Today 11, 46–50 (2008).
- 31 J. Guo, J.-T. Lü, Y. Feng, J. Chen, J. Peng, Z. Lin, X. Meng, Z. Wang, X.-Z. Li, E.-G. Wang, and Y. Jiang, "Nuclear quantum effects of hydrogen bonds probed by
- tip-enhanced inelastic electron tunneling," Science 352, 321–325 (2016). ³²S. R. Burema, K. Seufert, W. Auwärter, J. V. Barth, and M.-L. Bocquet, "Probing nitrosyl ligation of surface-confined metalloporphyrins by inelastic electron tunneling spectroscopy," ACS Nano 7, 5273-5281 (2013).
- 33 A. Erpenbeck and M. Thoss, "Hierarchical quantum master equation approach to vibronic reaction dynamics at metal surfaces," J. Chem. Phys. 151, 191101
- ³⁴A. Erpenbeck, Y. Ke, U. Peskin, and M. Thoss, "Current-induced dissociation in molecular junctions beyond the paradigm of vibrational heating: The role of antibonding electronic states," Phys. Rev. B 102, 195421 (2020).
- 35 Y. Ke, A. Erpenbeck, U. Peskin, and M. Thoss, "Unraveling current-induced dissociation mechanisms in single-molecule junctions," J. Chem. Phys. 154, 234702
- $^{\bf 36}$ K. J. Franke and J. I. Pascual, "Effects of electron–vibration coupling in transport through single molecules," J. Phys.: Condens. Matter 24, 394002 (2012).
- ³⁷R. Jorn and T. Seideman, "Implications and applications of current-induced dynamics in molecular junctions," Acc. Chem. Res. 43, 1186–1194 (2010). ³⁸D. Xiang, X. Wang, C. Jia, T. Lee, and X. Guo, "Molecular-scale electronics:
- From concept to function," Chem. Rev. 116, 4318-4440 (2016).
- ³⁹ J. K. Sowa and R. A. Marcus, "On the theory of charge transport and entropic effects in solvated molecular junctions," J. Chem. Phys. 154, 034110 (2021).
- ⁴⁰J. K. Sowa, J. A. Mol, G. A. D. Briggs, and E. M. Gauger, "Beyond Marcus theory and the Landauer-Büttiker approach in molecular junctions: A unified framework," J. Chem. Phys. 149, 154112 (2018).
- ⁴¹ M. Thoss and F. Evers, "Perspective: Theory of quantum transport in molecular junctions," J. Chem. Phys. 148, 030901 (2018).

 42G. Cohen and M. Galperin, "Green's function methods for single molecule
- junctions," J. Chem. Phys. **152**, 090901 (2020); arXiv:2001.06008.

 ⁴³ M. P. Das and F. Green, "Nonequilibrium mesoscopic transport: A genealogy,"
- Phys.: Condens. Matter 24, 183201 (2012).
- 44Y. Tanimura, "Numerically 'exact' approach to open quantum dynamics: The hierarchical equations of motion (HEOM)," J. Chem. Phys. 153, 020901 (2020).
- ⁴⁵O. Hod and L. Kronik, "The driven Liouville von Neumann approach to electron dynamics in open quantum systems," Isr. J. Chem. 63, e202300058 (2023)
- ⁴⁶R. Jorn and T. Seideman, "Theory of current-induced dynamics in molecular-
- scale devices," J. Chem. Phys. **124**, 084703 (2006).

 ⁴⁷R. Jorn and T. Seideman, "Competition between current-induced excitation and bath-induced decoherence in molecular junctions," J. Chem. Phys. 131, 244114 (2009).
- ⁴⁸N. Bode, S. V. Kusminskiy, R. Egger, and F. von Oppen, "Current-induced forces in mesoscopic systems: A scattering-matrix approach," Beilstein J. Nar technol. 3, 144-162 (2012).
- ⁴⁹A. Semenov and A. Nitzan, "Transport and thermodynamics in quantum
- junctions: A scattering approach," J. Chem. Phys. 152, 244126 (2020).

 50 U. Peskin, "An introduction to the formulation of steady-state transport through molecular junctions," J. Phys. B: At., Mol. Opt. Phys. 43, 153001 (2010).

- 51 V. May, "Electron transfer through a molecular wire: Consideration of electronvibrational coupling within the Liouville space pathway technique," Phys. Rev. B **66**, 245411 (2002).
- ⁵²J. Koch and F. von Oppen, "Franck-Condon blockade and giant Fano factors in transport through single molecules," Phys. Rev. Lett. 94, 206804 (2005); rXiv:0409667 [cond-mat].
- ⁵³R. Härtle and M. Thoss, "Resonant electron transport in single-molecule junctions: Vibrational excitation, rectification, negative differential resistance, and local cooling," Phys. Rev. B 83, 115414 (2011).
- ⁵⁴J. K. Sowa, N. Lambert, T. Seideman, and E. M. Gauger, "Beyond Marcus theory and the Landauer-Büttiker approach in molecular junctions. II. A self-consistent Born approach," J. Chem. Phys. 152, 064103 (2020).
- ⁵⁵G. Li, N. Govind, M. A. Ratner, C. J. Cramer, and L. Gagliardi, "Influence of coherent tunneling and incoherent hopping on the charge transfer mechanism in linear donor-bridge-acceptor systems," J. Phys. Chem. Lett. 6, 4889-4897 (2015).
- ⁵⁶M. Galperin, A. Nitzan, and M. A. Ratner, "Resonant inelastic tunneling in molecular junctions," Phys. Rev. B 73, 045314 (2006); arXiv:0510452 [cond-mat]. ⁵⁷F. Haupt, T. Novotný, and W. Belzig, "Phonon-assisted current noise in molecular junctions," Phys. Rev. Lett. 103, 136601 (2009); arXiv:09
- ⁵⁸R. Avriller and A. Levy Yeyati, "Electron-phonon interaction and full counting statistics in molecular junctions," Phys. Rev. B 80, 041309 (2009).
- ⁵⁹X. Dan, M. Xu, Y. Yan, and Q. Shi, "Generalized master equation for charge transport in a molecular junction: Exact memory kernels and their high order expansion," J. Chem. Phys. 156, 134114 (2022).
- ⁶⁰L. Kidon, H. Wang, M. Thoss, and E. Rabani, "On the memory kernel and the reduced system propagator," J. Chem. Phys. 149, 104105 (2018);
- ⁶¹ F. Evers, R. Korytár, S. Tewari, and J. M. van Ruitenbeek, "Advances and challenges in single-molecule electron transport," Rev. Mod. Phys. 92, 035001
- ⁶² J. Jin, X. Zheng, and Y. Yan, "Exact dynamics of dissipative electronic systems and quantum transport: Hierarchical equations of motion approach," J. Chem. s. 128, 234703 (2008); arXiv:0710.5
- $^{\bf 63}{\rm F.}$ Jiang, J. Jin, S. Wang, and Y. Yan, "Inelastic electron transport through mesoscopic systems: Heating versus cooling and sequential tunneling versus cotunneling processes," Phys. Rev. B 85, 245427 (2012).
- ⁶⁴R. Härtle, G. Cohen, D. R. Reichman, and A. J. Millis, "Decoherence and lead-induced interdot coupling in nonequilibrium electron transport through interacting quantum dots: A hierarchical quantum master equation approach," . Rev. B 88, 235426 (2013).
- ⁶⁵C. Schinabeck, A. Erpenbeck, R. Härtle, and M. Thoss, "Hierarchical quantum master equation approach to electronic-vibrational coupling in nonequilibrium transport through nanosystems," Phys. Rev. B 94, 201407 (2016).
- 66 H. Wang, I. Pshenichnyuk, R. Härtle, and M. Thoss, "Numerically exact, time-dependent treatment of vibrationally coupled electron transport in singlemolecule junctions," J. Chem. Phys. 135, 244506 (2011).
- ⁶⁷H. Wang, "Multilayer multiconfiguration time-dependent Hartree theory," s. Chem. A 119, 7951–7965 (2015).
- ⁶⁸L. Mühlbacher and E. Rabani, "Real-time path integral approach to nonequilibrium many-body quantum systems," Phys. Rev. Lett. 100, 176403 (2008).
- ⁶⁹L. Simine and D. Segal, "Path-integral simulations with fermionic and bosonic reservoirs: Transport and dissipation in molecular electronic junctions," J. Chem. Phys. 138, 214111 (2013).
- ⁷⁰G. Cohen, E. Gull, D. R. Reichman, A. J. Millis, and E. Rabani, "Numerically exact long-time magnetization dynamics at the nonequilibrium Kondo crossover of the Anderson impurity model," Phys. Rev. B 87, 195108 (2013); arXiv:1212.0546.
- H. Wang and M. Thoss, "A multilayer multiconfiguration time-dependent Hartree study of the nonequilibrium Anderson impurity model at zero
- temperature," Chem. Phys. **509**, 13–19 (2018). ⁷²J. Bätge, Y. Ke, C. Kaspar, and M. Thoss, "Nonequilibrium open quantum systems with multiple bosonic and fermionic environments: A hierarchical equations of motion approach," Phys. Rev. B 103, 235413 (2021); arXiv:2102.0948-
- 73 Y. Ke, R. Borrelli, and M. Thoss, "Hierarchical equations of motion approach to hybrid fermionic and bosonic environments: Matrix product state formulation in twin space," J. Chem. Phys. 156, 194102 (2022); arXiv:2202.10273.

- ⁷⁴Y. Ke, J. Dvořák, M. Čížek, R. Borrelli, and M. Thoss, "Current-induced bond rupture in single-molecule junctions: Effects of multiple electronic states and vibrational modes," J. Chem. Phys. 159, 024703 (2023).
- 75 Z. Jin and J. E. Subotnik, "Nonadiabatic dynamics at metal surfaces: Fewest switches surface hopping with electronic relaxation," J. Chem. Theory Comput. 17, 614-626 (2021).
- 76 N. Shenvi, S. Roy, and J. C. Tully, "Nonadiabatic dynamics at metal surfaces: Independent-electron surface hopping," J. Chem. Phys. 130, 174107 (2009).
- 77 W. Dou and J. E. Subotnik, "A broadened classical master equation approach for nonadiabatic dynamics at metal surfaces: Beyond the weak molecule-metal coupling limit," J. Chem. Phys. 144, 024116 (2016).

 78 W. Dou, C. Schinabeck, M. Thoss, and J. E. Subotnik, "A broadened
- classical master equation approach for treating electron-nuclear coupling in non-equilibrium transport," J. Chem. Phys. 148, 102317 (2018).
- ⁷⁹G. Miao, W. Ouyang, and J. Subotnik, "A comparison of surface hopping approaches for capturing metal-molecule electron transfer: A broadened classical master equation versus independent electron surface hopping," J. Chem. Phys. 150, 041711 (2019).
- ⁸⁰ M. Esposito and M. Galperin, "Transport in molecular states language: Generalized quantum master equation approach," Phys. Rev. B 79, 205303 (2009). ⁸¹W. Dou, A. Nitzan, and J. E. Subotnik, "Surface hopping with a manifold of
- electronic states. II. Application to the many-body Anderson-Holstein model," Chem. Phys. 142, 084110 (2015).
- 82 F. Ramírez, D. Dundas, C. G. Sánchez, D. A. Scherlis, and T. N. Todorov, "Driven Liouville-von Neumann equation for quantum transport and multipleprobe Green's functions," J. Phys. Chem. C 123, 12542–12555 (2019).

 83 M. Galperin and A. Nitzan, "Nuclear dynamics at molecule–metal interfaces: A
- pseudoparticle perspective," J. Phys. Chem. Lett. 6, 4898–4903 (2015).

 84 A. Ben-Reuven and S. Mukamel, "Comments on the formal theory of scattering
- and relaxation," J. Phys. A: Math. Gen. 8, 1313-1327 (1975).
- 85 R. F. Snider, "Relaxation and transport of molecular systems in the gas phase," Int. Rev. Phys. Chem. 17, 185-225 (1998).
- ⁸⁶ A. Ben-Reuven, "Spectral line shapes in gases in the binary-collision approximation," Adv. Chem. Phys. 33, 235–293 (1975).
- E. Mulvihill and E. Geva, "A road map to various pathways for calculating the memory kernel of the generalized quantum master equation," J. Phys. Chem. B 125, 9834-9852 (2021).
- $^{\bf 88}{\rm Q}.$ Shi and E. Geva, "A new approach to calculating the memory kernel of the generalized quantum master equation for an arbitrary system-bath coupling," Chem. Phys. 119, 12063-12076 (2003).
- ⁸⁹ A. Szabo and N. S. Ostlund, Modern Quantum Chemistry: Introduction to
- Advanced Electronic Structure Theory, 1st ed. (Dover, Mineola, NY, 1996).

 90 S. Yeganeh, M. A. Ratner, M. Galperin, and A. Nitzan, "Transport in state space: Voltage-dependent conductance calculations of benzene-1,4-dithiol," Nano Lett. 9, 1770-1774 (2009).

- ⁹¹ R. Jorn and T. Seideman, "Dissipation in molecular junctions," J. Chem. Phys. 129, 194703 (2008).
- 92 S. Mukamel, Principles of Nonlinear Optical Spectroscopy, 1st ed. (Oxford University Press, New York, 1995).
- ⁹³S. Nakajima, "On quantum theory of transport phenomena," Prog. Theor. Phys. 20, 948-959 (1958).
- ⁹⁴R. Zwanzig, "Ensemble method in the theory of irreversibility," J. Chem. Phys. **33**, 1338-1341 (1960).
- 95 R. F. Snider and J. G. Muga, "Properties of the transition superoperator," Can. J. Phys. 72, 152-161 (1994).
- 96 Y. Hu and S. Mukamel, "Tunneling versus sequential long-range electron transfer: Analogy with pump-probe spectroscopy," J. Chem. Phys. 91, 6973-6988 (1989).
- 97 R. D. Levine, Quantum Mechanics of Molecular Rate Processes, 1st ed. (Dover Publications, Mineola, NY, 1969).
- 98 R. F. Snider, "Quantum-mechanical modified Boltzmann equation for degenerate internal states," J. Chem. Phys. 32, 1051-1060 (1960).
- ⁹⁹M. Sparpaglione and S. Mukamel, "Dielectric friction and the transition from adiabatic to nonadiabatic electron transfer in condensed phases. II. Application to non-Debye solvents," J. Chem. Phys. 88, 4300-4311 (1988).
- 100 A. P. Jauho, N. S. Wingreen, and Y. Meir, "Time-dependent transport in interacting and noninteracting resonant-tunneling systems," Phys. Rev. B 50, 5528-5544 (1994).
- ¹⁰¹ A. Erpenbeck, C. Hertlein, C. Schinabeck, and M. Thoss, "Extending the hierarchical quantum master equation approach to low temperatures and realistic band structures," J. Chem. Phys. 149, 064106 (2018).

 102 E.-D. Fung, D. Gelbwaser, J. Taylor, J. Low, J. Xia, I. Davydenko, L. M. Campos,
- S. Marder, U. Peskin, and L. Venkataraman, "Breaking down resonance: Nonlinear transport and the breakdown of coherent tunneling models in single molecule
- junctions," Nano Lett. 19, 2555–2561 (2019).

 103 C. S. Lau, H. Sadeghi, G. Rogers, S. Sangtarash, P. Dallas, K. Porfyrakis, J. Warner, C. J. Lambert, G. A. D. Briggs, and J. A. Mol, "Redox-dependent Franck-Condon blockade and avalanche transport in a graphene-fullerene
- single-molecule transistor," Nano Lett. 16, 170–176 (2016).

 104 D. J. Scalapino and S. M. Marcus, "Theory of inelastic electron-molecule interactions in tunnel junctions," Phys. Rev. Lett. 18, 459-461 (1967).
- ¹⁰⁵G. Binnig, N. Garcia, and H. Rohrer, "Conductivity sensitivity of inelastic scanning tunneling microscopy," Phys. Rev. B 32, 1336–1338 (1985).
- 106B. N. J. Persson and A. Baratoff, "Inelastic electron tunneling from a metal tip: The contribution from resonant processes," Phys. Rev. Lett. 59, 339-342
- (1987).

 107 U. Fano, "Pressure broadening as a prototype of relaxation," Phys. Rev. 131,
- 108 J. R. Taylor, Scattering Theory: The Quantum Theory of Nonrelativistic Collisions (Robert E. Krieger Publishing Company, Malabar, FL, 1972).